

**DEPOSITIONAL ENVIRONMENTS AND PARAGENETIC
POROSITY CONTROLS, UPPER RED RIVER
FORMATION, NORTH DAKOTA**

by
W. Kipp Carroll

REPORT OF INVESTIGATION NO. 66
NORTH DAKOTA GEOLOGICAL SURVEY
Lee C. Gerhard, State Geologist
1979

**DEPOSITIONAL ENVIRONMENTS AND PARAGENETIC
POROSITY CONTROLS, UPPER RED RIVER
FORMATION, NORTH DAKOTA**

by

W. Kipp Carroll

**REPORT OF INVESTIGATION NO. 66
NORTH DAKOTA GEOLOGICAL SURVEY**

Lee C. Gerhard, State Geologist

1979

TABLE OF CONTENTS

	Page
LIST OF ILLUSTRATIONS	v
ACKNOWLEDGMENTS	vii
ABSTRACT	1
INTRODUCTION	1
Previous Work	3
Tectonic Setting and History	6
Purpose	6
Methods	6
“D” ZONE	9
Facies and Stratigraphy	9
Environmental Interpretation	9
Diagenetic Fabrics	13
Diagenetic Mechanisms	16
Porosity Development	23
“A,” “B,” AND “C” ZONES	23
Facies and Stratigraphy	23
Environmental Interpretation	31
Diagenetic Fabrics	31
Diagenetic Mechanisms	32
Porosity Development	35
DISCUSSION	35
HYDROCARBON PRODUCTION AND POTENTIAL	38
Past and Current Production	38
Potential for Production	38
CONCLUSIONS	39
REFERENCES CITED	40
APPENDIX A. Well Location Index	43
APPENDIX B. Well Log Picks of Tops of Units within the Upper Red River	47

LIST OF ILLUSTRATIONS

Figure	Page
1. Outline of main part of Williston basin, and areal distribution of the Red River Formation	2
2. Upper Red River stratigraphic column	4
3. North Dakota Paleozoic stratigraphic column	5
4. Regional isopach of Red River Formation	7
5. Approximate locations of structures affecting Upper Red River sedimentation	8
6. Idealized "D" zone stratigraphic column	10
7. Core slab of "D" zone burrowed facies, with minimum diagenetic alteration	11
8. Core slab of "D" zone organic facies, showing typical laminated character	11
9. Core slab of wispy laminated dolomitic mudstone that occasionally occurs interbedded with the two major "D" zone facies	11
10. Approximate area in which well logs indicate the presence of at least some alternating succession of "D" zone facies	12
11. Photomicrograph of desiccation fractures in the "D" zone burrowed facies (plane polarized light)	13
12. Interpreted depositional setting of "D" zone, based upon possible contemporary analog, Laguna Mormona, Baja, Mexico	14
13. Flow diagram of paragenesis in the "D" zone burrowed facies	15
14. Photomicrograph of dolomitized burrows, showing "V" fractures (plane polarized light)	17
15. Photomicrograph of dolomitized burrows, showing coalesced dolomite aureoles and hollow burrow centers (plane polarized light)	17
16. Photomicrograph of second stage dolomite partially filling cavity in the center of a dolomitized burrow (plane polarized light)	17
17. Photomicrograph of large dolomite rhombs "floating" in the mud matrix	17
18. Photomicrograph of stylolites outlining dolomitized burrows (plane polarized light)	18
19. Photomicrograph of fossils in organic units that have been dissolved and replaced with microspar	18
20. Sequence of core slab photographs top to bottom in a burrowed unit of the "D" zone, showing progressive dolomitization and calcite solution down-section	19
21. Photomicrograph of lowest horizon of a burrowed unit in the "D" zone, showing the remaining first and second stage dolomite after pervasive calcite solution	20

Figure	Page
22. Interpreted lateral and vertical relationships of dolomitizing solutions and sedimentary facies in the "D" zone	21
23. Core slab of basal wacke-packstone	25
24. Photomicrograph of intraclastic, skeletal, sparry packstone	25
25. Core slab of wispy laminated, porous dolomitic mudstone	26
26. Photomicrograph of desiccation fractures	26
27. Photomicrograph of acicular anhydrite crystals in dolomitic mudstone (plane polarized light)	27
28. Photomicrograph of subaerial laminated crust in dolomitic mudstone	27
29. Photomicrograph of pelletal packstone fabric in dolomitic mudstone	27
30. Photomicrograph of cut and fill structure with associated intraclasts in dolomitic mudstone (plane polarized light)	27
31. Core slab of undolomitized mudstone	28
32. Core slab of thinly bedded dolomitic mudstone	28
33. Core slab of possible algal mats in dolomitic mudstone	28
34. Photomicrograph of possible algal mats in dolomitic mudstone	28
35. White, very fine-grained, chalky dolomitic mudstone	29
36. Core slab of nodular anhydrite	29
37. Core slab of nodular anhydrite and thinly bedded anhydrite	29
38. Areal distribution of "C," "B," and "A" anhydrite units	30
39. Photomicrograph of pinpoint porosity in dolomitic mudstone	33
40. Photomicrograph of secondary dolomite lining vugs in dolomitic mudstone (plane polarized light)	33
41. Circulation pattern of dolomitizing solutions in the "A," "B," and "C" porosity	34
42. Idealized diagram of Upper Red River sedimentation through time	36
Plates	
1. Isopach—Upper Red River	(in pocket)
2. Structure Contour—Red River Top	(in pocket)
3. North-South and West-East Cross Sections	(in pocket)
4. Isopach—Upper Red River: "D" Zone Through "C" Anhydrite	(in pocket)

ACKNOWLEDGMENTS

I gratefully acknowledge the guidance, assistance, and critical reviews of Dr. Lee C. Gerhard and Dr. Timothy A. Cross, and review of the manuscript by Dr. Odin D. Christensen. The North Dakota Geological Survey made available logs, and other data, and Chevron Oil Company, Consolidated Interstate Gas, Farmers Union Central Exchange, Inc., Webb Resources, Inc., and the North Dakota Geological Survey provided financial support for this research.

ABSTRACT

The upper Red River Formation in North Dakota comprises a subtidal/intertidal facies overlain by three evaporitic sequences of four lithologic units each, labeled "C," "B," and "A" in stratigraphic order. Four porosity zones are recognized in the upper Red River: the subtidal/intertidal facies forms one porosity zone, and each evaporitic sequence contains another. Each unit in a sequence, as well as the sequence itself, is thinner and less widespread than its preceding counterpart. All strata are laterally continuous across the main part of the Williston basin in North Dakota, but the porosity zones eventually disappear to the east as they approach the basin margin. Porosity within any given zone varies from one part of the basin to another, often within relatively short distances.

The "D" porosity zone consists of two primary lithologic facies: a shallow subtidal burrowed mudstone and skeletal wackestone, and an impermeable, often laminated, black organic skeletal wackestone and packstone deposited in an intertidal or supratidal barred pond environment. Porosity in the subtidal burrowed facies is due to syndepositional dolomitization and later calcite solution and microfracturing. Maximum porosity values related to dolomitization and calcite dissolution occur in the burrowed horizons immediately above the impermeable organic units, which acted as barriers to interstitial fluid movement. Poor development of the organic units near the center of the basin perhaps accounts for sporadic porosity development in that area.

The basal unit of each of the sequences overlying the "D" zone consists of open shelf bioturbated skeletal wackestone of characteristically low porosity. Porous, fine-grained, primary supratidal dolomite overlies the subtidal facies, and these units form the "C," "B," and "A" porosity zones. A very thin argillaceous marker bed of non-calcareous shale completes each sequence.

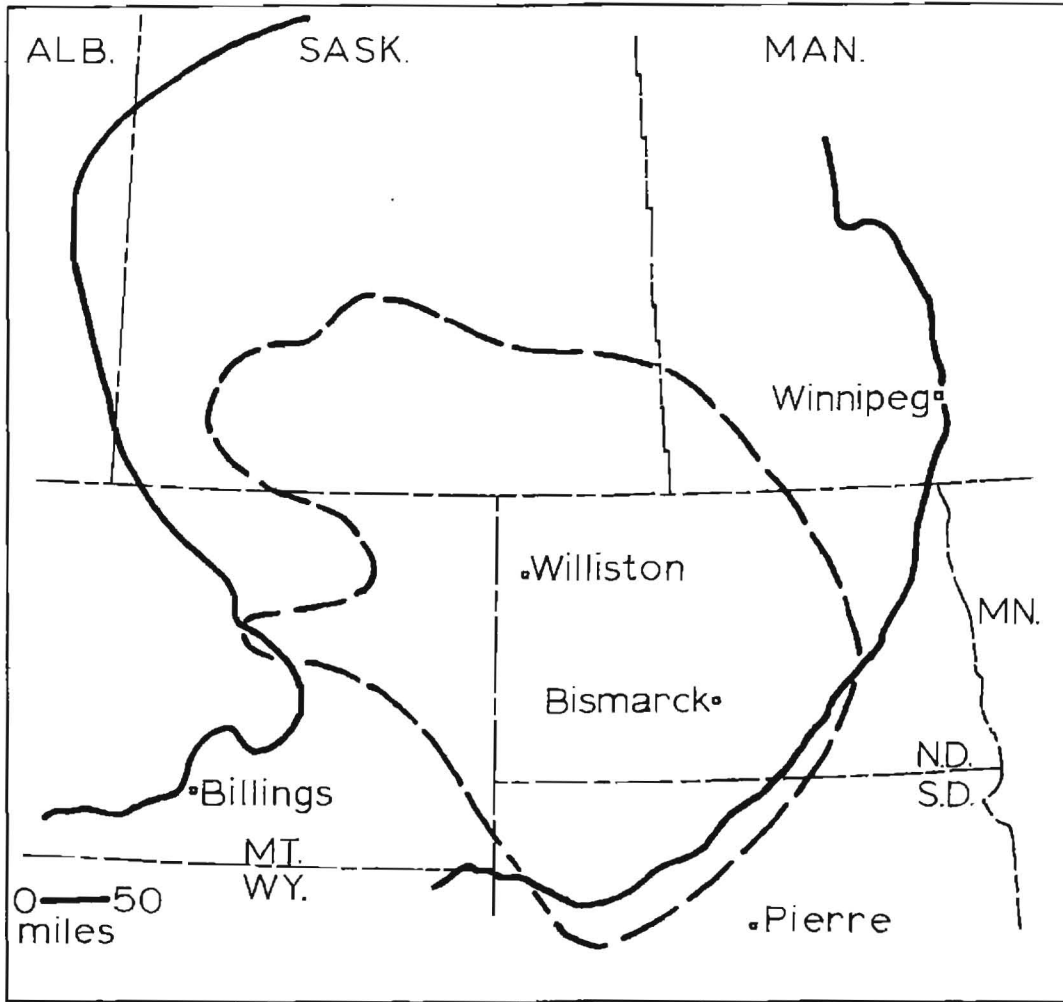
Porosity in the supratidal dolomite stems from intercrystalline voids and pinpoint porosity due to solution. Porosity in the upper three zones varies across the basin and is directly related to degree of exposure of the sediment in the supratidal environment, during which dolomitization occurred.

INTRODUCTION

The Red River Formation (Middle to Upper Ordovician) is present throughout the Williston basin (fig. 1). Maximum thickness of slightly over 700 feet occurs in the central part of the basin in Dunn County, North Dakota. Most of the original thickness of the formation is preserved in the basin center in North Dakota and along the western periphery in Montana, but has been thinned by erosion to a feather edge at the eastern periphery of the basin in eastern North Dakota. The Red River Formation is recognized in Manitoba, Saskatchewan, North Dakota, and the Williston basin portions of Montana and South Dakota. Equivalent strata in other areas of Montana and Wyoming form the lower portion of the Bighorn Group. In Kansas, Oklahoma, and Nebraska the Viola and Fernvale Formations are correlative units (Fuller, 1961). In the Black Hills area of South Dakota the Whitewood dolomite comprises the lower part of the Red River.

Various stratigraphic subdivisions of the Red River Formation have been proposed. The most widely used is the upper/lower terminology (Sinclair, 1959; Fuller, 1961; Ballard, 1963; Friestad, 1969), which is used in this report.

The Red River Formation consists predominantly of limestone and dolomitic limestone. Red River carbonates rest conformably on clastics of the Middle Ordovician Winnipeg Formation. Throughout most of the basin a series of argillaceous layers, the Hecla beds (Fuller, 1961), occur as a 10- to 40-foot-thick transition at the base of the Red River. Contact with shale of the overlying Stony Mountain Formation is abrupt but conformable. In the central portion of the Williston basin the Stony Mountain shale, the lowest member of the Stony Mountain Formation, is absent and the top of the Red River is defined as a thin argillaceous layer five to twenty feet above the uppermost evaporite bed (Fuller, 1961).



- areal distribution of Red River Formation
- - - Williston basin

Figure 1. Outline of main part of Williston basin, and areal distribution of the Red River Formation (Modified from Carlson and Anderson, 1965; and Mallory, 1972).

The lower Red River comprises at least two-thirds of the formation, ranging from 400 to 550 feet thick. In the central basin, the basal part of the lower Red River consists of fossiliferous, bioturbated wackestone characterized by a mottled texture due to selective dolomitization. Toward the margin of the basin this unit becomes less fossiliferous and less mottled and grades into dense microgranular brown dolomites with occasional vugs. The upper part of the lower Red River consists of porous, fossiliferous, medium to fine-grained dolomitic wackestone that grades into dense, microgranular and lithographic dolomite near the margin of the basin (Porter and Fuller, 1959).

Maximum upper Red River thickness of 275 feet occurs in the basin center in Dunn County. The section includes four porosity zones, labeled "D" through "A" in stratigraphic order, separated by impermeable units of skeletal wacke-packstone and anhydrite (fig. 2). The "D" zone consists of variably dolomitized, stylolitic, burrowed,* skeletal mudstone and wackestone (terminology of Dunham, 1962). Non-porous, fossiliferous organic packstone units are interbedded with porous strata of the "D" zone.

Above the "D" zone, an ordered sequence of four lithologic units is repeated three times in vertical section. In stratigraphic order each sequence consists of (1) impermeable, mottled, slightly dolomitic, bioturbated fossiliferous wackestone, (2) porous, laminated, fine-grained brown dolomitic mudstone, often containing small euhedral anhydrite crystals, (3) impermeable nodular anhydrite, and (4) a thin argillaceous bed that corresponds to a gamma ray log characteristic traceable throughout the basin. These three similar depositional episodes were labeled the "P," "R," and "F" rhythms by Fuller (1961, table 1). Through common usage, the dolomitic mudstone units contained in these rhythms have been referred to as the "C," "B," and "A" porosity zone, respectively.

A final unit of mottled, dolomitic, bioturbated skeletal wackestone, resembling the basal unit of each sequence, overlies the uppermost argil-

*In this paper, a distinction is made between "burrowed" and "bioturbated." Burrowed refers to primary fabrics in which the sediment has not been homogenized by biologic activity and individual, discrete burrows can be identified. Bioturbated refers to primary fabrics in which no individual burrows can be discerned, but biologic activity has completely reworked and homogenized the sediment.

laceous marker and comprises the remainder of the upper Red River. In most wells studied, each sequence and each unit within a sequence is thinner than its preceding counterpart. In addition, the anhydrite units become progressively less widespread in each successive sequence. All three anhydrite units, however, are present in the basin center. The argillaceous marker at the top of the lowest sequence persists across the basin, but the upper two markers are less persistent and usually cannot be discerned on logs toward the periphery of the basin.

Previous Work

Foerste (1929) first applied the name "Red River Formation" to the carbonate sequence between the Winnipeg and Stony Mountain Formations, and divided it into the Dog Head, Cat Head, and Selkirk members. Porter and Fuller (1959) divided the formation into a lower unit of fossiliferous, dolomitic limestone, and an upper unit of cyclically deposited evaporites and carbonates; each cycle was subdivided into basal limestone, fine-grained dolomite, and anhydrite. Baillie (1952) noted that the Dog Head, Cat Head, and Selkirk divisions that Foerste (1929) described in Lake Winnipeg outcrops are not traceable as such into the subsurface. Andrichuk (1959) formulated subsurface divisions that include a basal limestone, an intermediate dolomitic limestone and secondary dolomite, and an upper dolomite. Fuller (1961) and the Canadian Geological Survey (Sinclair, 1959) proposed a two unit division: a lower, variably dolomitized, marine fossiliferous limestone that includes about five-sixths of the thickness of the formation, and an upper section restricted to the basin interior that is evaporitic, thinly bedded, and of uniform thickness. Subsequent reports (Ballard, 1963; Friestad, 1969) support this two unit division.

Early investigators assigned both Richmondian (Bassler, 1915; Hussey, 1926; Foerste, 1928) and Trentonian (Whiteaves, 1897; Dowling, 1900; Kay, 1935; Flower, 1952) ages to the Red River Formation on the basis of paleontological evidence. On the basis primarily of brachiopods, the Red River was restricted to Richmondian age (Macauley and Leith, 1951; Twenhofel, 1954; Ross, 1957). On the basis of graptolites, Patterson (1961, fig. 7) shows the Red River as equivalent to Viola (Middle Ordovician) and Bighorn as equivalent to Middle and Upper Ordovician. The Red River is shown as Middle to Upper

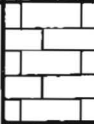

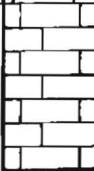


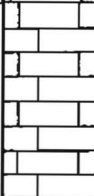



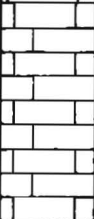

Fuller, 1961	This Report			
				gray, bioturbated, skeletal wacke-packstone
F Rhythm	"A" Sequence	porous zone		argillaceous marker nodular anhydrite
				brown, fine-grained dolomitic mudstone
				gray, bioturbated, skeletal wacke-packstone
R Rhythm	"B" Sequence	porous zone		argillaceous marker nodular anhydrite
				brown, fine-grained dolomitic mudstone
				gray, bioturbated, skeletal wacke-packstone
P Rhythm	"C" Sequence			argillaceous marker nodular anhydrite
		porous zone		brown, fine-grained dolomitic mudstone
				gray, bioturbated, skeletal wacke-packstone
	"D" porosity zone			interbedded brown, dolomitic, burrowed wackestone and black, organic packstone

Figure 2. Upper Red River stratigraphic column.

Sequence	System	Group or Formation
Absaroka	Permian	Spearfish
		Winnekahta
		Opeche
	Pennsylvanian	Minnelusa
		Amsden
Kaskaskia	Mississippian	Big Snowy Group
		Madison
		Bakken
	Devonian	Three Forks
		Birdbear
		Duperow
		Souris River
		Dawson Bay
		Prairie
		Winnipegosis
	Silurian	Interlake
		Stonewall
		Stony Mountain
Winnipeg		
Deadwood		
Sauk	Cambrian	Deadwood

Figure 3. North Dakota Paleozoic stratigraphic column.

Ordovician on the correlation chart in the Geologic Atlas of the Rocky Mountain Region (Mallory, 1972, p. 77).

Tectonic Setting and History

The Williston basin is an intracratonic basin that forms the major structural feature in North Dakota and large parts of Saskatchewan, Manitoba, and South Dakota (fig. 1). Basin subsidence began in the Middle Ordovician (Sandberg, 1964), resulting in a shallow depression in which sand and shale of the Winnipeg Formation were deposited. Rate of subsidence increased and at the time of Red River sedimentation the basin was connected with the open ocean to the west (fig. 4). During lower Red River deposition the basin's center, as indicated by maximum stratigraphic thickness, was in Oliver County in west-central North Dakota. The depositional center subsequently migrated northwest and during upper Red River sedimentation was in northeastern Dunn County. At present, the structural center of the basin is about 40 miles southeast of Williston, North Dakota.

Several structural or topographic features affected Red River sediment distribution as evidenced by thinning and thickening of Red River strata over the positive and negative relief areas respectively (fig. 5). A break in basin slope, sometimes referred to as the basin hinge line (Ballard, 1963), also produced a significant effect on sedimentation. This feature strikes north-south along 101° W. longitude and is concave toward the main part of the basin to the west. The hinge line marks a pronounced change from gently westward dipping strata on the basin's eastern flank to more steeply dipping strata in the basin proper. In addition, all Red River strata thin rapidly as they approach the hinge line from the west (Ballard, 1963). The lowest of the three anhydrite beds is present east of the hinge line and the depositional limits of the upper two lie at or west of the hinge line. The porous, fine-grained dolomites of the upper two depositional sequences ("A" and "B") merge approximately at the hinge line, but the porous dolomite of the "C" sequence may be traced separately for some distance farther east.

The north-south trending Nesson anticline in northwestern North Dakota was a prominent positive structural and topographic feature throughout the Paleozoic. Red River strata thin

over the anticline forming combined structural and stratigraphic traps.

In Bowman County the Cedar Creek anticline existed as a topographic high, but except for small structural highs on the anticline itself, the feature was apparently inactive during the late Ordovician. Upper Red River strata maintain relatively constant thickness across the anticline.

Local thickness changes shown by an isopach map of the formation (pl. 1), indicate a number of minor structures that had less pronounced effects on Red River sedimentation. The Billings nose forms a prominent north-south trending structure in Billings County. The Divide low is a shallow depression in Divide County. The Emmons and Stutsman highs, in counties of the same name, are sub-circular structures of 20 to 30 feet maximum relief. The Burleigh high is a low relief structure elongate in a north-south direction. A relatively large high may exist in the Hettinger-Stark-Morton County area, but insufficient well control precludes defining it. Ballard (1963) suggests highs in Mercer, Ward, and Foster Counties similar to the Emmons and Stutsman highs. Upper Red River strata are unusually thick in Wells County, indicating a low area.

Comparison of isopach (pl. 1) and structure contour maps (pl. 2) indicates that topographic expression of most of the above features was eliminated by Red River sedimentation. Therefore, with the exception of the Nesson anticline and perhaps the Billings nose, the structures were inactive during and after Red River deposition.

Purpose

The purpose of this study is to (1) reconstruct depositional environments through microfacies and regional lithofacies analysis, (2) describe the types and origins of porosity within the upper Red River, and (3) explain the causes of localization of porosity development within the upper Red River. Depositional environment of the sediments and subsequent paragenesis constitute the two major elements investigated as factors responsible for porosity development.

Methods

This study concentrates primarily on examination of well cores and logs held by the North Dakota Geological Survey. As most cores are

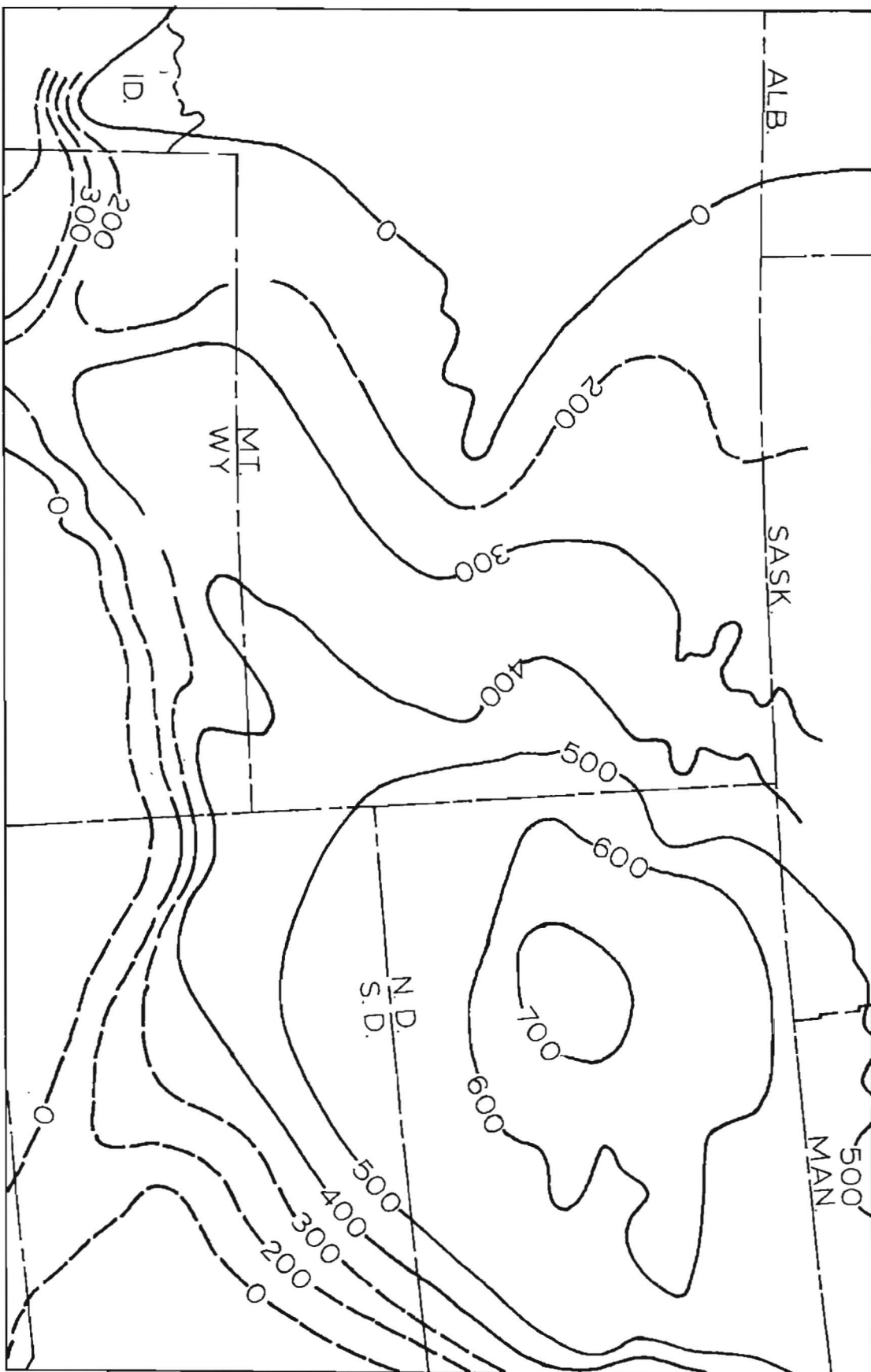
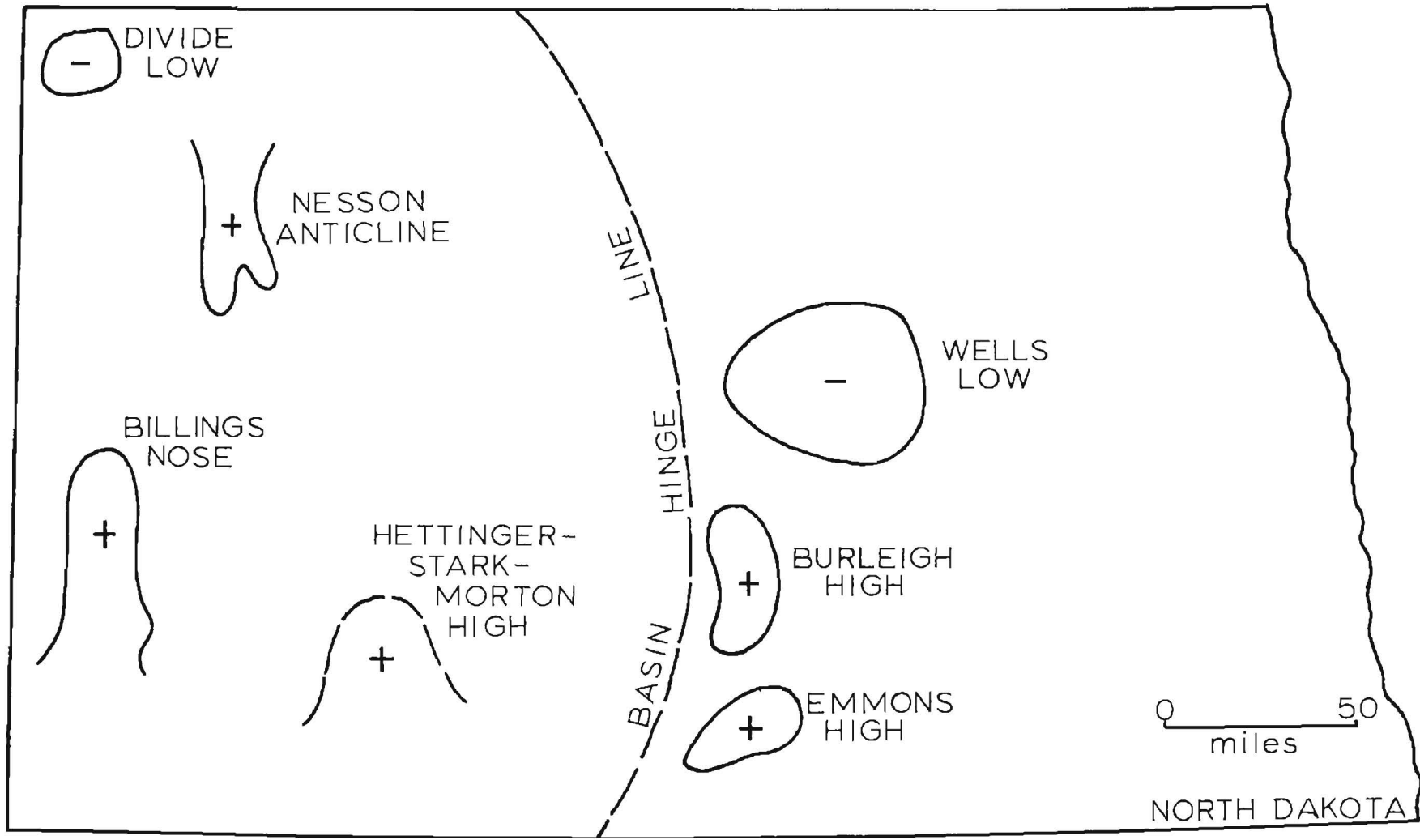


Figure 4. Regional isopach of Red River Formation (Modified from Mallory, 1972, p. 82).



(+) positive elements (-) negative elements

Figure 5. Approximate locations of structures affecting upper Red River sedimentation.

from wells in western North Dakota, it was necessary to rely on logs for stratigraphic correlation and facies interpretation in the central and eastern areas. Data analysis and interpretation are based on 213 well logs, 28 cores, and more than 500 petrographic thin sections.

Description of regional stratigraphy and major lithofacies of the upper Red River was accomplished by reconnaissance core study. Selected slabs, thin sections, and acetate peels were examined for constituent particles, mineralogy, and primary and secondary fabrics. These analyses, combined with lateral and vertical facies relationships, permitted reconstruction of paleo-depositional environments. Diagenetic history of all units was investigated, with emphasis on the known porosity zones. In addition to petrography, other techniques utilized for detailed study of the paragenesis included insoluble residue analysis, staining, X-ray diffraction, and cathodoluminescence.

"D" ZONE

Facies and Stratigraphy

The base of the "D" zone is chosen as the base of the upper Red River. The zone ranges from 50 feet thick, where identifiable near the edge of the basin, to a maximum of about 70 feet in the basin depocenter in Dunn County. It is continuous across the main part of the basin in North Dakota, and can be traced for varying distances onto the eastern flank (pl. 3).

In Bowman County, the "D" zone is comprised of a sequence of two regularly interbedded primary facies (fig. 6). Units ranging from 5 to 23 feet thick of partially dolomitized, porous, burrowed brown mudstone and skeletal wackestone (fig. 7) are overlain by units 2 to 5 feet thick of impermeable, often laminated, slightly argillaceous, black organic skeletal wackestone and packstone (fig. 8). Abundant black organic material, occurring as dense laminations approximately 1 mm thick and as small dispersed flecks, characterizes these later units. Some of this organic material may have a kerogen-like character as suggested by Kendall (1974). White grainstone layers one to three inches thick occur intermittently within the organic beds and are sharply contrasted to the normally dark color of the units. Beds of dolomitic mudstone (fig. 9) one to four feet thick occur in addition to the two

dominant "D" zone facies, either immediately above or below an organic unit.

The regular succession of the two dominant "D" zone facies as diagrammed in figure 6 can be identified in cores and on logs along most of the margin of the main basin in North Dakota (fig. 10), but lack of cores prevents determination of exact lateral limits of its development. The succession is poorly developed in the center and deepest part of the basin, and usually is not present east of the basin hinge line. The zone is thickest at the center of the basin, but is comprised predominantly of the burrowed facies. Although present, units of the impermeable organic facies are not well developed nor as numerous in the basin center as toward the edge of the basin proper where five distinct units are recognized. The fine-grained dolomitic mudstone is present in the center of the basin in only one well.

Kendall (1974, p. 132) photographically illustrated "D" zone cores from southern Saskatchewan that bear a remarkable resemblance to cores of the same zone from Bowman County, North Dakota. Although he does not describe in detail the stratigraphic succession in that area, his photographs demonstrate that both the burrowed and organic facies are developed in the shallow part of the Williston basin to the north.

Environmental Interpretation

The burrowed wackestone fabric represents very shallow subtidal to low intertidal deposition. Infrequent desiccation fractures (fig. 11) indicate occasional subaerial exposure, probably of short duration. These units differ from underlying lower Red River strata and the basal unit of the overlying sequence in that individual discrete burrows, elongate and semicircular in cross-section, are prominent in the "D" zone. By contrast, in the units above and below the "D" zone, bioturbation has completely homogenized the sediment and no individual burrows are discernible. Also in the "D" zone burrowed facies, fossil fragments are less abundant (mudstone to wackestone fabric) than in the overlying and underlying strata (generally wackestone to packstone fabrics).

The differential degree of sediment reworking (burrowed versus bioturbated character) of the "D" zone burrowed facies relative to overlying and underlying strata may be a response to some change in biologic activity or physical conditions. The discrete burrows of the "D" zone may have

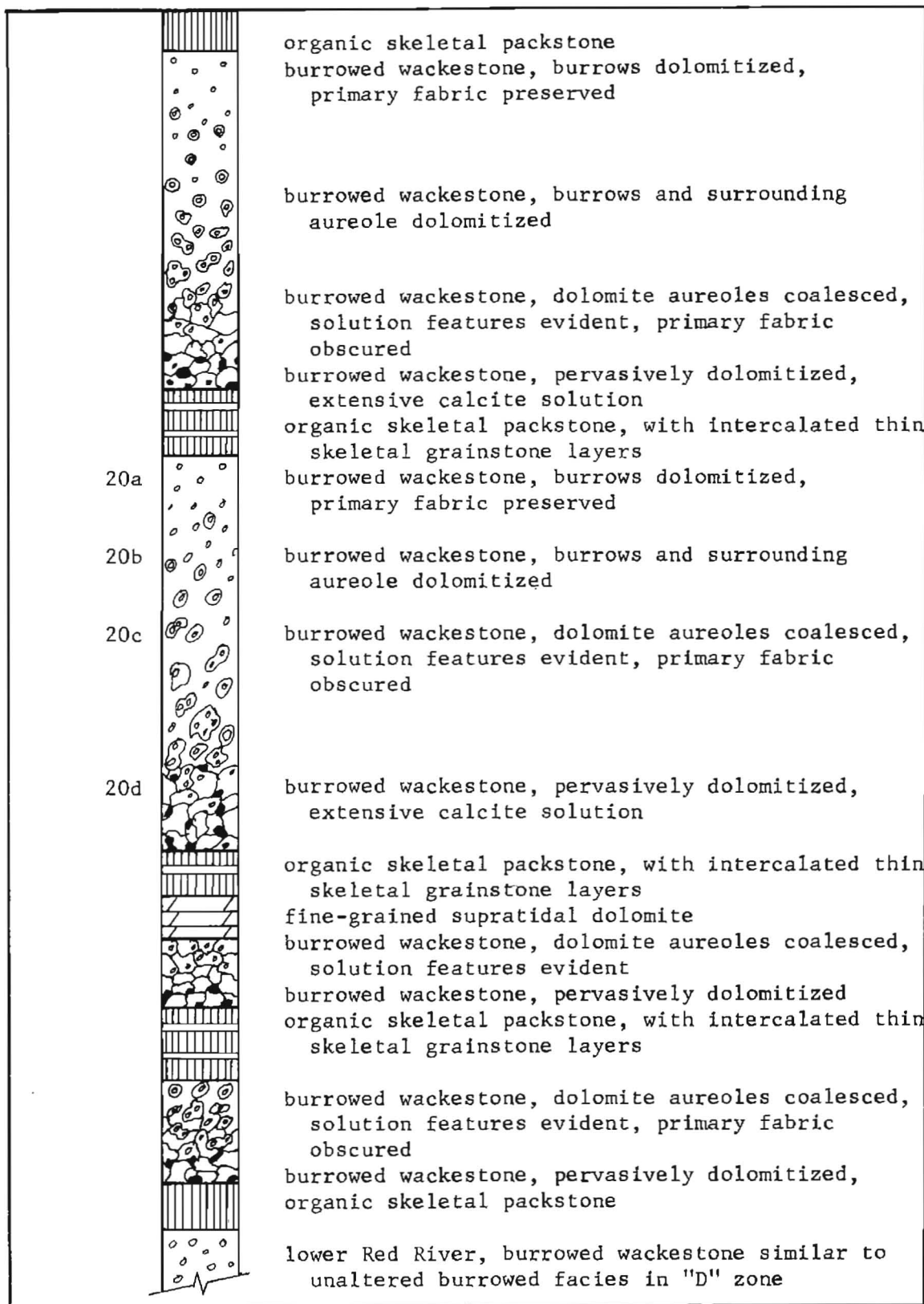


Figure 6. Idealized "D" zone stratigraphic column. Numbers to left of column correspond to figure of the same number.

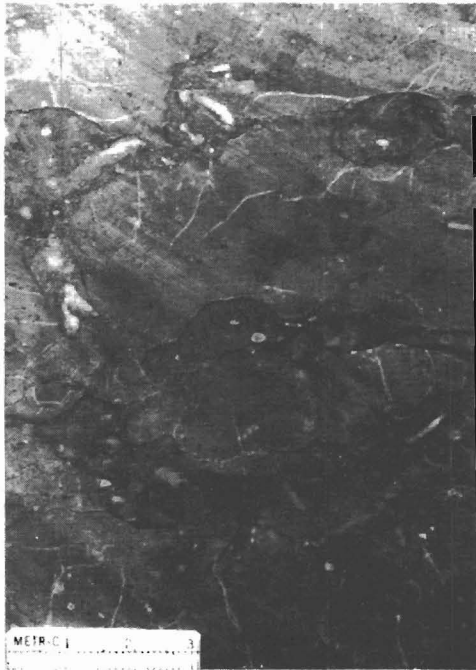


Figure 7. Core slab of "D" zone burrowed facies, with minimum diagenetic alteration.

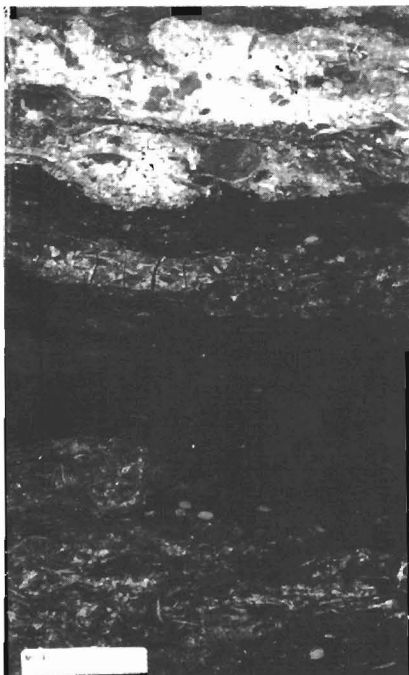


Figure 8. Core slab of "D" zone organic facies, showing typical laminated character. Note the light colored grainstone layers near the top of the photo.



Figure 9. Core slab of wispy laminated dolomitic mudstone that occasionally occurs interbedded with the two major "D" zone facies.

been produced by a different assemblage of organisms than existed in the more thoroughly reworked strata. Alternatively, fewer and more discrete burrows may reflect a reduced biologic density relative to that in the subadjacent and supra-adjacent strata. Higher salinity, shallower water, reduced circulation, or a combination of these factors may be the parameters that controlled the organisms or their activities responsible for the different fabrics.

Preservation of abundant organic detritus in the organic skeletal packstone units indicates some restriction of circulation. Sulfide minerals are not found in these units; therefore, while circulation may have been restricted, reducing conditions did not prevail. Deposition in a barred, intertidal to supratidal saline pond and evaporite flat environment is proposed for these beds (fig. 12). The area behind the bar probably was restricted from circulation with the open ocean and periodically inundated with sea water. Evaporation increased salinity in this broad pond or flat and a restricted fauna, principally algae and infaunal grazers, resulted in limited reworking of the sediment. Although algal mat filaments are not preserved, abundant organic detritus and laminated sediment suggests prolific development of algal mats on the sediment surface of the shallow pond. Occasional storms or high spring tides breached the barriers and reflooded the ponds with sea water, carrying in abundant normal marine shells and fragments and orienting them preferentially to the flow. Periodic storms or high tides also explain the grainstone layers within the organic units.

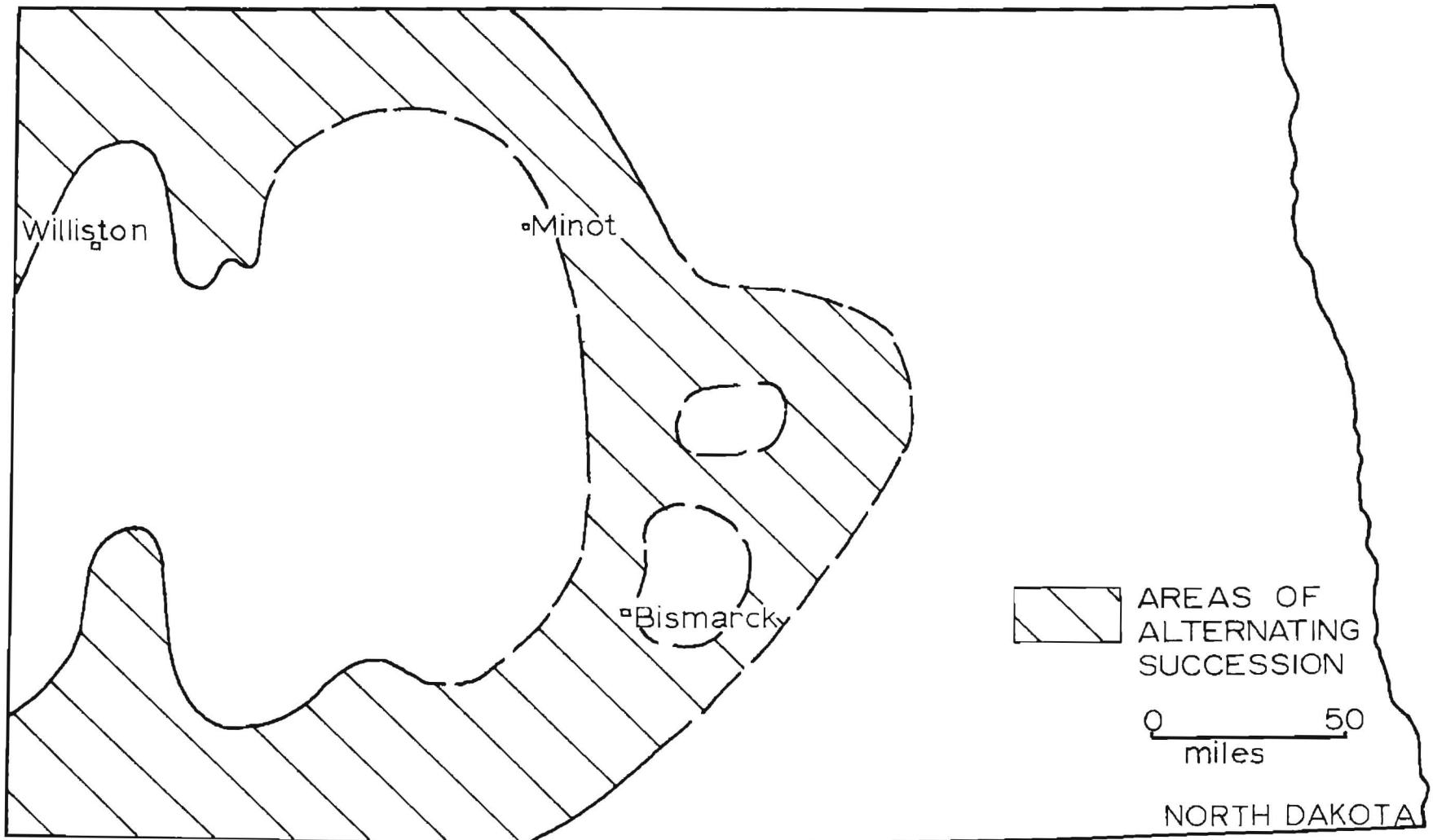


Figure 10. Approximate area in which well logs indicate the presence of at least some alternating succession of "D" zone facies.

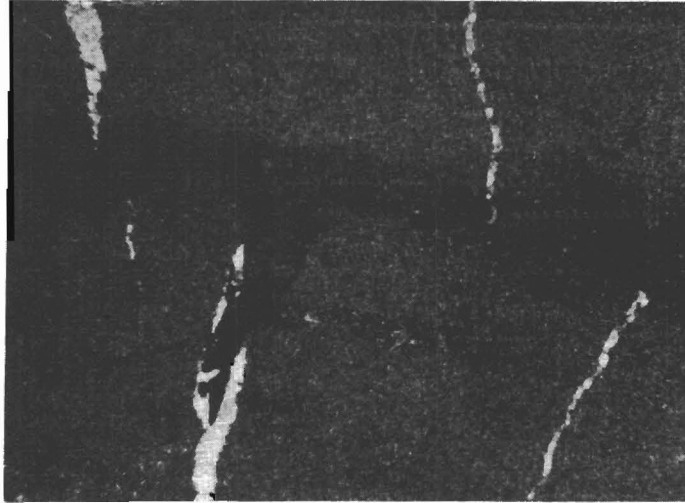


Figure 11. Photomicrograph of desiccation fractures in the "D" zone burrowed facies (plane polarized light).

A modern analog of this inferred deposition setting may exist at Laguna Mormona, Baja, Mexico (Horodyski, Bloeser and Vonder Haar, 1977; Horodyski and Vonder Haar, 1975) or the salt ponds on St. Croix, U.S.V.I. (personal observation, 1975). These ponds are approximately at sea level, are completely restricted from the open ocean by subaerially exposed dunes or bars, and are periodically flooded during storms when the barriers are breached. A very limited fauna inhabits these ponds due to high salinity and temperature, but algal mats proliferate. Shallow coring in Laguna Mormona demonstrates that discrete algal mats are not preserved greater than 10 cm below the sediment surface, but the sediment is highly organic and faintly laminated.

The fine-grained dolomitic mudstone that is sometimes present in the "D" zone is a supratidal deposit similar to the porous rocks comprising the overlying "A," "B," and "C" zones. These mudstones may represent an evaporitic flat landward of the ponds that was generally not preserved.

In Bowman County, five repetitions of the subtidal burrowed facies overlain by the intertidal, barred pond organic facies can be demonstrated in at least five cores. The base of the "D" zone, and thus the base of the upper Red River, is usually picked on logs at the lowest organic unit because porosity in the underlying burrowed facies is poorly developed due to factors considered in the following discussion. This lowest burrowed facies is gradational with the underlying lower Red River.

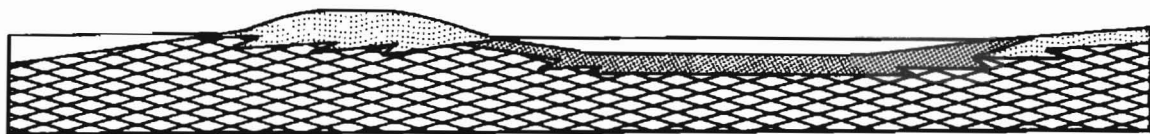
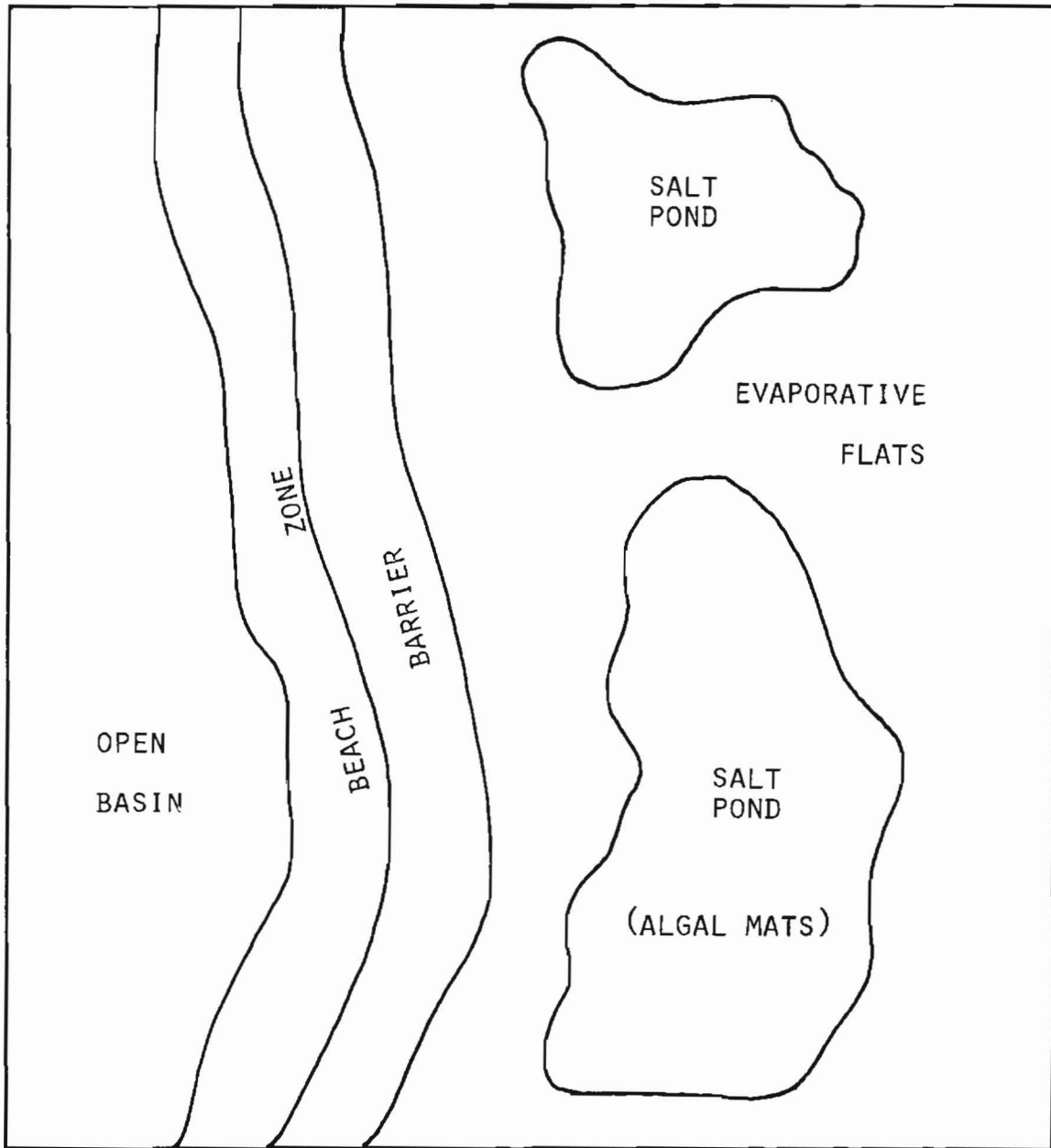
The laterally extensive and continuous nature

of the subtidal burrowed facies indicates that the North Dakota part of the Williston basin was normally covered by very shallow water. Depositional environments were uniform from the center of the basin to the margins, where the character of the sediment changed from the subtidal burrowed facies to the barred intertidal pond organic facies. No rocks indicative of deeper water deposition are found, even at the center of the basin. As a result of the extremely low depositional slope, extensive lateral migration of one facies over another occurred commonly in response to minor sea level fluctuations, variations in rates of sediment accumulation, or both. Differential rates of sediment accumulation could be a result of storm deposition, current activity, or varying rates of physicochemical and biologic production of carbonate.

Diagenetic Fabrics

Several stages of diagenesis are recognized in the "D" zone, the chronology of which was determined by cross-cutting relationships (fig. 13). Each stage resulted in different recognizable characteristics, some of which caused porosity enhancement and others porosity occlusion.

The primary fabric of the burrowed facies was modified by three essentially syndepositional diagenetic processes. Dolomitization replaced the original micrite filling the burrows and, in many instances, an aureole of sediment surrounding them. "V"-shaped fractures developed radially from the centers of the dolomitized burrows (fig. 14). The open ends of these fractures terminate at the edge of the dolomite, indicating that they






-  burrowed facies
-  organic facies
-  supratidal facies

Figure 12. Interpreted depositional setting of "D" zone, based upon possible contemporary analog, Laguna Mormona, Baja, Mexico.

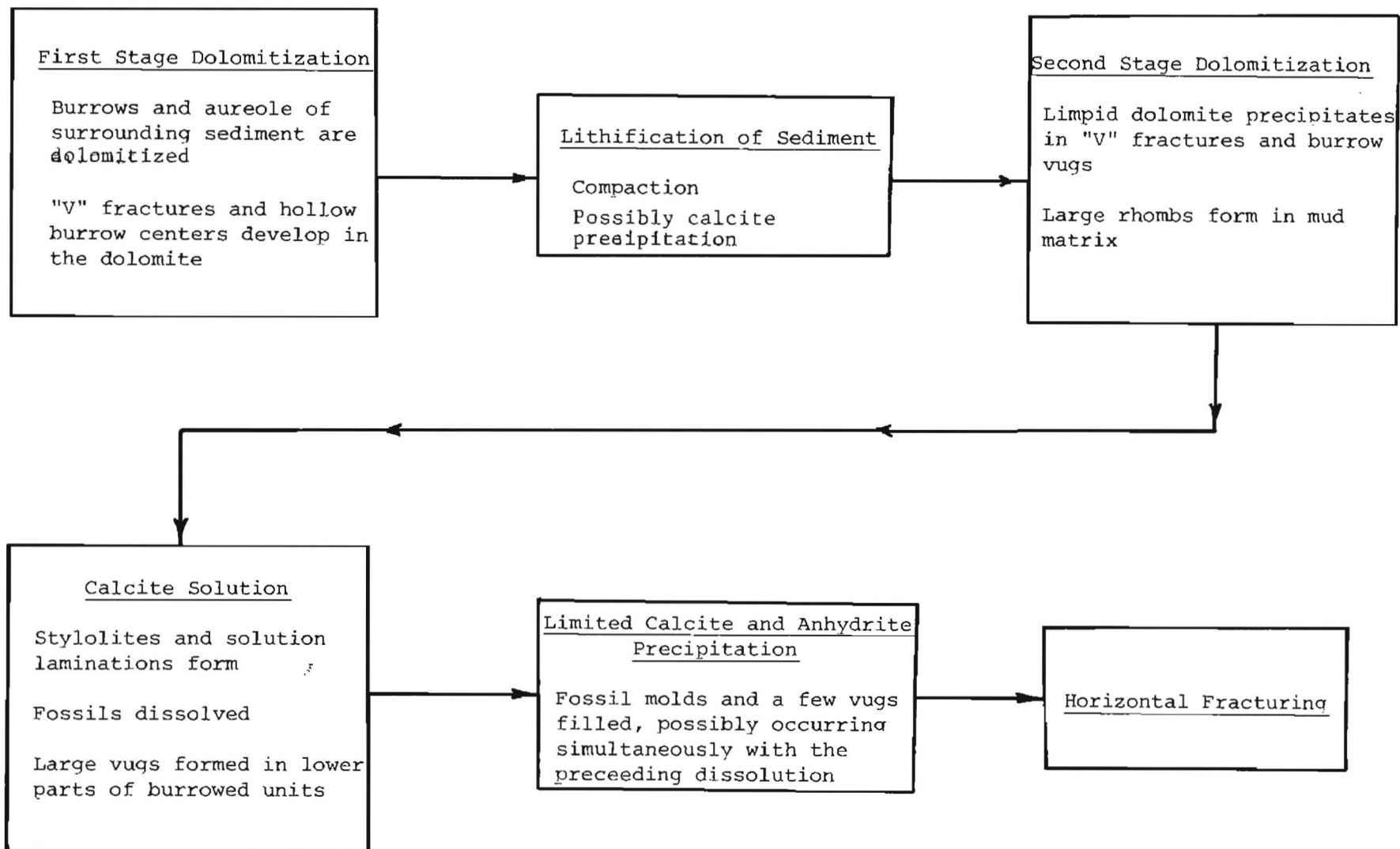


Figure 13. Flow diagram of paragenesis in the "D" zone burrowed facies.

developed prior to lithification of the enclosing sediment. In addition to the "V" fractures, a circular vug often formed in the dolomite at the center of a burrow. Where dolomite aureoles are developed, the entire burrow is sometimes hollow (fig. 15). Following these alterations, the main body of sediment was lithified.

A second, post-lithification stage of dolomitization ensued, forming larger, clearer (limpid) crystals than produced by the first stage dolomitization. This second stage dolomite partially or completely fills the "V" fractures and voids at the centers of burrows (fig. 16). Large euhedral dolomite rhombs occur "floating" in the micrite matrix of the burrowed facies (fig. 17). These rhombs have an irregular distribution, though perhaps are more prolific near the base of each burrowed unit. These crystals are neither as cloudy as the first stage nor as clear as the second stage dolomite. Correspondence in size with the second stage dolomite suggests coeval formation.

Post-lithification and post-dolomitization solution of a substantial percentage of the skeletal fragments created fossil-moldic porosity. Abundant stylolites and solution laminations were also formed. These latter two features often outline dolomitized burrows or their aureoles, and in some instances truncate second stage dolomite (fig. 18).

Precipitation of calcite spar and minor quantities of anhydrite in many of the remaining burrow vugs, fossil molds, and "V" fractures resulted in approximately 20 to 50 percent porosity occlusion. Both minerals occur in single thin sections; however, it has not been possible to ascertain the order of precipitation. Spar and anhydrite precipitation probably was penecontemporaneous with stylolitization.

Horizontal fracturing is the final stage of diagenesis, as these fractures cut across all other features. All such fractures observed are open, though in some cases minor quantities of microspar line the fracture walls. This fracturing is assumed to have occurred much later in the history of the rock, after stylolitization.

Diagenetic processes had considerably less effect on the organic units of the "D" zone than on the burrowed strata. In all cases, the primary fabric of the organic beds is easily discerned. Solution of many fossil fragments is the most apparent alteration, resulting in molds that have been refilled with spar or microspar (fig. 19). Stylolites occur in these beds, but are not as

abundant as in the burrowed facies. This stylolitization, dissolution, and precipitation in vugs is considered to be a result of the same process responsible for similar features in the burrowed facies. Dolomitization in the organic beds is limited, and usually is associated with organic laminations. This may be a result of high initial Mg content in the organic matter (Gebelein and Hoffman, 1973). The organic units probably became impermeable shortly after deposition and initial burial due to compaction, oriented (flat-lying) fossils, organic laminations, high organic content, and presence of argillaceous material.

Increased diagenetic alteration and progressively greater porosity downsection can be demonstrated in each of the four burrowed facies in the "D" zone (fig. 6). Progressive increase in amount of first stage dolomitization and more thorough dissolution of calcite toward the base of each unit occurs in all cases studied, and is most apparent in the thicker units. Near the top of a burrowed unit the primary rock fabric is preserved; usually only the burrows are dolomitized (fig. 20a). The main body of sediment was unaffected, presumably a result of preferential flow of intrastratal fluids through the burrows due to their greater primary porosity. First stage dolomitization increases downsection to include: (1) aureoles of dolomitized sediment immediately surrounding burrows (fig. 20b), (2) coalescence of aureoles (fig. 20c), and (3) immediately above the underlying organic bed, pervasive dolomitization which completely obscures the primary rock fabric (fig. 20d). Virtually no calcite solution occurs near the top of a burrowed unit, whereas at the base, elongate or irregularly shaped vugs up to 1 cm in diameter and 5 cm in length are present. In many instances calcite solution at the base of a burrowed unit is so complete that only poorly cemented first and second stage dolomite crystals remain (fig. 21).

Diagenetic Mechanisms

First stage dolomitization occurred by mixing of fresh and sea water in the phreatic zone of the intertidal environment (fig. 22). Astronomic tides and minor sea level fluctuations induced by barometric pressures and wind stress (Illing, Wells and Taylor, 1965; Kerr and Thomson, 1963) caused extensive ebb and flow across broad tidal flats. When the flats were flooded, sea water percolated into the sediment preferentially through the more porous burrows and mixed with

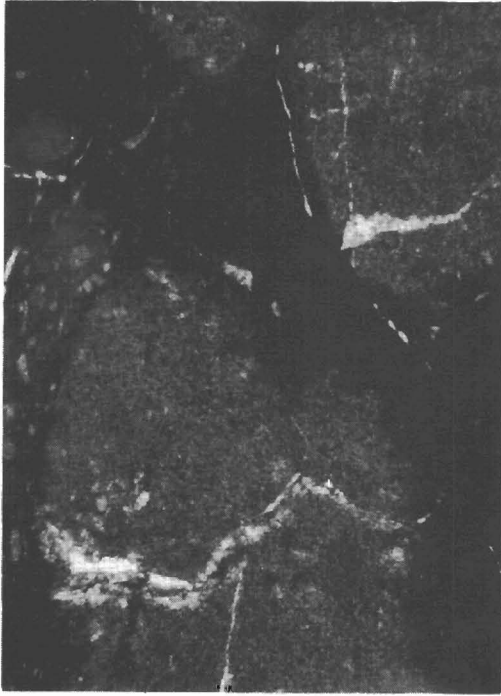


Figure 14. Photomicrograph of dolomitized burrows, showing "V" fractures (plane polarized light).



Figure 15. Photomicrograph of dolomitized burrows, showing coalesced dolomite aureoles and hollow burrow centers (plane polarized light).

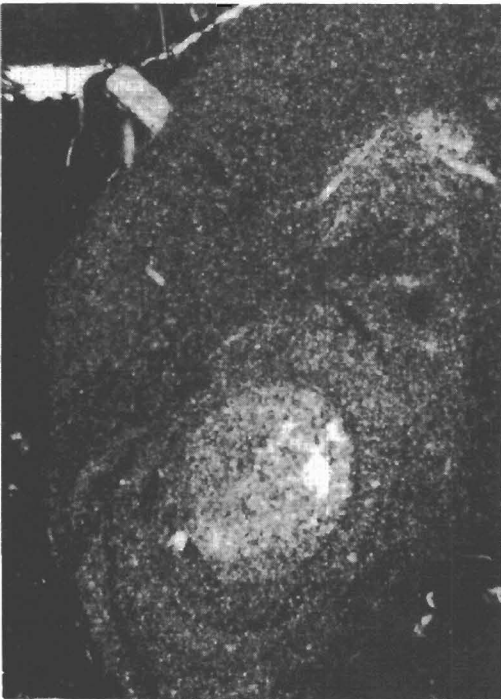


Figure 16. Photomicrograph of second stage dolomite partially filling cavity in the center of a dolomitized burrow (plane polarized light).

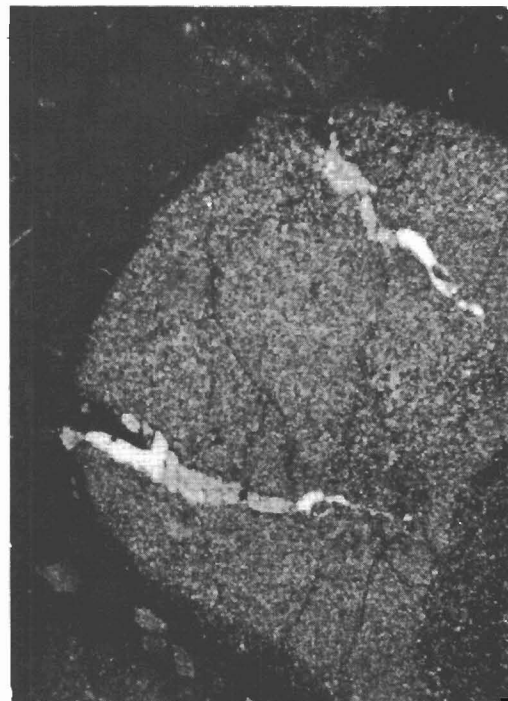


Figure 17. Photomicrograph of large dolomite rhombs "floating" in the mud matrix. Also note the mud that "dripped" into the "V" fractures before the mud was lithified, and the second stage dolomite that partially fills the "V" fractures (plane polarized light).

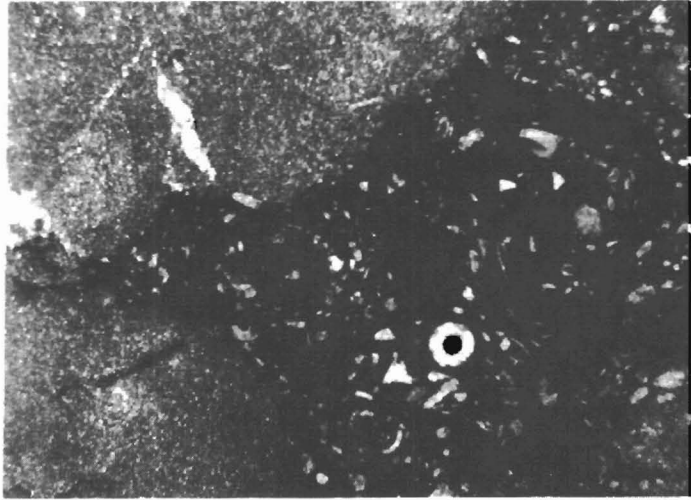


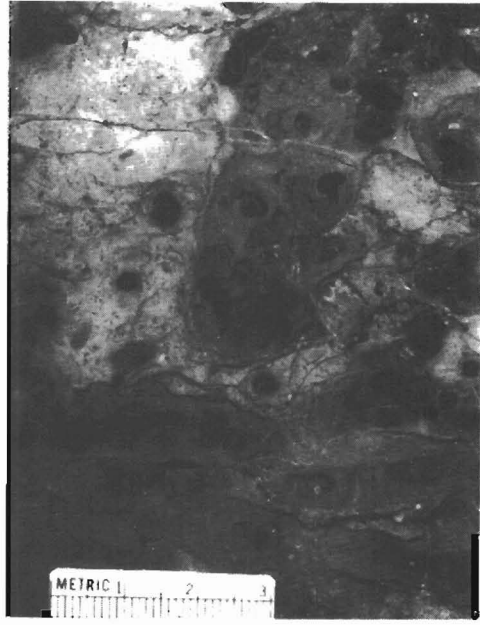
Figure 18. Photomicrograph of stylolites outlining dolomitized burrows (plane polarized light).



Figure 19. Photomicrograph of fossils in organic units that have been dissolved and replaced with microspar. Also note the organic laminations (plane polarized light).



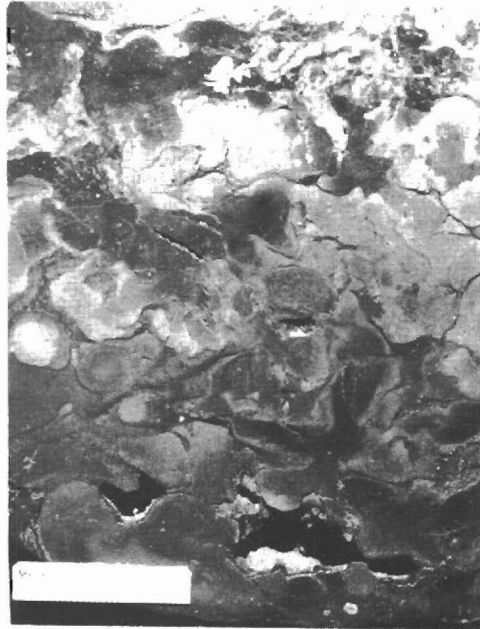
Figure 20. Sequence of core slab photographs top to bottom in a burrowed unit of the "D" zone, showing progressive dolomitization and calcite solution down-section.
 (a) burrows dolomitized, some dolomite aureoles developed, low porosity, primary fabric essentially intact.



(b) dolomite aureoles coalesced, some solution laminations that outline dolomitized areas, limited porosity.



(c) more thorough dolomitization than in (b), solution laminations, porous, primary fabric obscured.



(d) pervasive dolomitization, solution vugs and laminations, primary fabric completely obscured, excellent porosity.

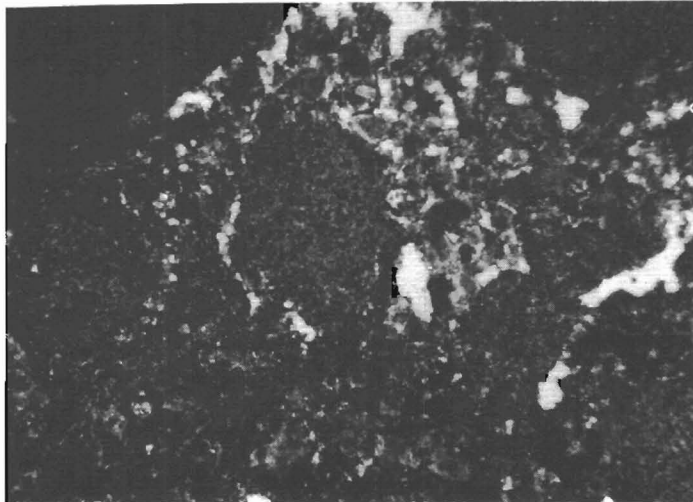


Figure 21. Photomicrograph of lowest horizon of a burrowed unit in the "D" zone, showing the remaining first and second stage dolomite after pervasive calcite solution. White areas are voids (plane polarized light).

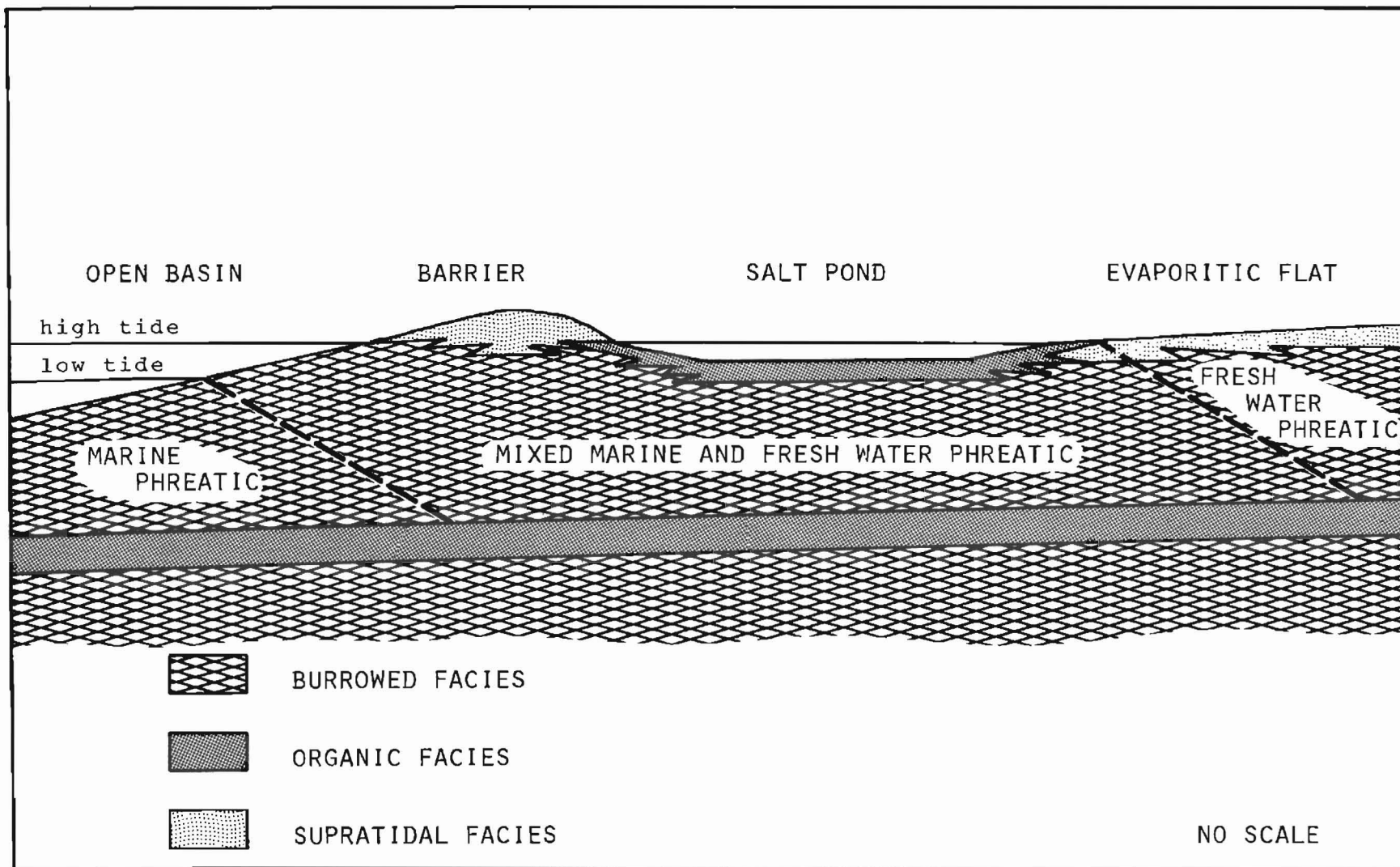


Figure 22. Interpreted lateral and vertical relationships of dolomitizing solutions and sedimentary facies in the "D" zone.

the continental fresh water lens. As noted by Badiozamani (1973), fresh water dilution of marine water reduces salinity and raises the Mg/Ca ratio; dolomitization occurs when Mg/Ca approaches a 1:1 ratio providing there is a concomitant reduction of salinity (Folk and Land, 1975). It is proposed that first stage dolomitization of near surface sediments occurred penecontemporaneously with sedimentation in the intertidal or very shallow subtidal zone as a consequence of periodic mixing of fresh and marine waters. First stage dolomitization was limited to the sediment above the underlying organic unit, due to the impermeability of that unit. Thus, the zone of mixed fresh and marine phreatic waters was effectively perched. The most extensive mixing, and therefore the most dolomitization, occurred immediately above this organic bed where variable surface conditions had the least effect. More dolomitization also occurs at the base of a burrowed unit due to greater residence time of the well-mixed fresh and sea waters. The sediment-water interface was the upper edge of the mixing zone, but the sediment at the surface was alternately flushed with sea water and fresh water, resulting in very little mixing and reduced dolomitization.

Interstitial movement of dolomitizing fluids also seems to enhance dolomitization (Deffeyes, Lucia and Weyl, 1965; Hanshaw, Back and Deike, 1971; Folk and Land, 1975). Two mechanisms may have acted to move the sea water-fresh water mixed zone. Rising tide caused sea water to infiltrate the sediment and raise the water table, and the hydrostatic head of this higher water table forced the fresh water lens and the mixing zone landward. As the tide ebbed, the fresh water hydrostatic head pushed the mixing zone seaward. Depending upon the magnitude of the tides or sea level fluctuations induced by barometric pressure and wind stresses, and permeability of the sediment, lateral movement of the mixing zone could have been considerable over the broad, low relief tidal flats. Movement of the mixing zone was also controlled by the size of the fresh water lens. As the size and thereby the hydrostatic pressure of the fresh water lens increased, the mixed water was forced seaward. Movement of the mixing zone as a result of this mechanism was probably a seasonal phenomenon.

First stage dolomitization of a burrowed unit was terminated by deposition of the overlying organic bed, which due to its low permeability

reduced or cut off the supply of dolomitizing fluids. Termination of first stage dolomitization in a particular burrowed unit was therefore essentially simultaneous with cessation of deposition of that unit. The mixing zone was now perched on the overlying organic unit, and began dolomitizing sediment in the next overlying burrowed unit as it was deposited.

Replacement of calcite by dolomite can result in a 12 to 13 percent volume reduction (Landes, 1946; Murray, 1960; Weyl, 1960). The "V" fractures in the dolomitized burrows probably formed during first stage dolomitization as shrinkage fractures resulting from this volume reduction. The small vugs at the centers of dolomitized areas are also attributed to the dolomitization process; whereas the path of greatest flow of the dolomitizing fluid was the burrow, and sediment surrounding this path was dolomitized, sediment within the burrow itself was dissolved. No positive proof of this mechanism can be demonstrated; however, a similar phenomenon has been observed on a larger scale in Bermuda (F. T. McKenzie, personal communication, 1978). An alternative explanation is that dolomite in the burrows was dissolved after termination of first stage dolomitization in the "D" zone and normal sea water again flooded the area.

Lithification of the main body of sediment followed first stage dolomitization probably as a result of compaction and calcite cementation.

Second stage dolomitization occurred after lithification of the main body of sediment and probably after deposition of the overlying evaporites ("C" zone and its associated anhydrite). Fresh continental water percolated downward and seaward through the underlying "D" zone strata and mixed with the normal marine intrastratal water in "D" zone vugs and fractures. Limpid dolomite precipitated in these voids, in a process similar to the mixed sea water-fresh water (Dorag) mechanism of Badiozamani (1973). The large euhedral rhombs floating in the mud matrix also formed at this time. It has not been possible to establish rhomb development in a chronological relationship with other features in the rocks, other than that they are probably post-lithification and prestylolization. Folk and Land (1975) have suggested that large, relatively clear (limpid) crystals of dolomite form slowly. Inasmuch as formation of fine-grained dolomite is inferred as a relatively rapid, syndepositional process, second stage dolomitization is considered

to be responsible for the larger, euhedral, limpid rhombs. Apparent increase in the number of rhombs toward the base of some of the burrowed units is probably due to later solution of calcite, causing the dolomite rhombs to become more closely packed together.

Subsequent calcite dissolution which created stylolites, fossil molds, and vugs probably resulted from subaerial exposure of the basin following each period of evaporite deposition, as well as during later, more prolonged periods of subaerial exposure such as at the end of the Silurian. During these exposures, fresh water percolating through the rocks dissolved calcite mud matrix and fossil fragments. Intrastratal flow in the "D" zone was intensified in the lower parts of the burrowed units immediately above each impermeable organic bed, and therefore maximum dissolution occurred at these horizons. As the solution became saturated, calcite precipitated in molds and vugs within the burrowed wackestone until the solution was again undersaturated with respect to calcite. This process probably recurred with each exposure of the basin. Probably during the times of calcite precipitation, anomalous conditions related to the solutions or the enclosing strata caused minor quantities of anhydrite to precipitate.

Horizontal fracturing occurred at a later but undetermined time. In Bowman County, any of several later movements along the Cedar Creek anticline may be responsible. The cause of fractures elsewhere in the basin is unknown.

Porosity Development

Porosity in the burrowed facies developed due to diagenetic changes of the primary rock fabric. The paragenesis outlined indicates at least five instances of porosity enhancement; first stage dolomitization, "V" fracturing and formation of vugs in burrows, formation of fossil molds and vugs through calcite dissolution, and horizontal fracturing. Partial porosity occlusion resulted from precipitation of second stage dolomite in "V" fractures and vugs, and calcite and anhydrite precipitation within secondary solution vugs and fossil molds. The intercrystalline porosity that developed during first stage dolomitization and the later vugs developed during solution of the calcite matrix, particularly near the base of each burrowed unit, account for most existing porosity.

Porosity development in many cases is controlled by small topographic highs over pre-existing structures approximately 2 to 5 miles wide and 3 to 10 miles long that exist throughout the basin. These local highs are reflected by depositional thins that form many productive structural-stratigraphic traps in North Dakota. These features are most apparent in Bowman County where well control is best, but limited suggests similar features. Porosity in the "D" zone is best developed on the flanks of these positive elements, while the tops of the structures often lack adequate porosity for hydrocarbon production. One explanation for this situation is that as the mixing zone oscillated, dolomitizing solutions followed the easiest path of flow, going around rather than over the highs. The same deflection of flow occurred with vug-forming solutions. As a result, crests of topographic highs have undergone less dolomitization and less calcite dissolution than the adjacent strata along their flanks.

In the center of the basin, "D" zone porosity is frequently poor and erratic in occurrence. This may be explained by the sporadic occurrence of organic-rich impermeable beds in the basin center; in absence of laterally continuous impermeable barriers, intrastratal solutions were not vertically confined to horizontal planes of flow and, instead, flow was more diffuse throughout the "D" zone. Lack of an impermeable barrier beneath the lowest burrowed unit, generally considered to be below the "D" zone, also accounts for its poorly developed porosity despite a primary fabric identical to the overlying porous units.

"A," "B," AND "C" SEQUENCES

Facies and Stratigraphy

The "A," "B," and "C" sequences of the upper Red River resulted from three similar depositional episodes and are treated together in this paper. A succession of three distinct lithologic facies comprise each of the three depositional sequences: basal wacke-packstone, overlain by dolomitic mudstone, capped by nodular anhydrite (fig. 2).

The basal unit of each sequence is a light to dark gray, slightly dolomitic, bioturbated, sparse skeletal wackestone to packstone (fig. 23). Groups of brown to black, sub-parallel and sub-horizontal wavy laminations of organic detritus are abundant throughout these units. Brachiopods, echinoderms (predominantly crinoids), bry-

ozoans, trilobites, and occasional corals (predominantly rugose) characterize the fossil assemblage. As a rule, these strata are impermeable, though small solution vugs are occasionally present. Near the top of many of the wacke-packstone units, clear microspar rather than micrite constitutes a large percentage of the matrix material (fig. 24). Such beds usually have packstone rather than wackestone fabrics, contain abundant mudstone intraclasts, and are gradational with the underlying wackestone. Thin horizons of sparry packstone also occasionally occur interspersed through the wackestone.

Fine-grained, dolomitized brown mudstone with good intercrystalline porosity overlies the basal wacke-packstone (fig. 25). These porous dolomitic mudstones form the actual "A," "B," and "C" zone reservoirs. These units contain desiccation features (fig. 26), abundant individual and massed acicular anhydrite crystals (fig. 27), subaerial laminated crust (fig. 28), pelletal fabrics (fig. 29), and erosional surfaces with associated intraclasts (fig. 30). Although these strata consist principally of fine-grained dolomite, primary sedimentary fabrics, for example, the fine laminations in figure 26, are clearly preserved. Interbedded with the fine-grained dolomitic mudstone are occasional horizons of undolomitized micrite (fig. 31) showing the same primary mudstone fabric as is preserved in dolomitized horizons. Both dolomitized and undolomitized strata vary from wispy laminated and almost featureless rocks (fig. 32), to densely laminated horizons which may be algal mats (figs. 33, 34). Infrequent burrows usually are more thoroughly dolomitized and contain slightly larger dolomite crystals than the enclosing sediment. Gastropods and brachiopods are the most common constituents of the very sparse fossil assemblage. Near the base of the units, fossil content often increases and the rocks are predominantly wackestones. In three cores studied, the Depco, Inc.—Hughes 13-27 in Bowman County, the Lion Oil Co.—Erickson 1 in Bottineau County and the Pure Oil Co.—J. M. Carr 1 in Foster County, the "B" zone is represented by a white, sometimes vuggy and poorly cemented, very fine-grained chalky dolomite (fig. 35).

Impermeable nodular anhydrite and interlaminated anhydrite and dolomite overlie the fine-grained dolomitic mudstones and comprise the third unit of each sequence (figs. 36, 37). In a number of wells in Bowman County, including the

well containing the chalky white dolomite, the dolomitic mudstones do not have anhydrite caps.

An argillaceous marker bed immediately on top of each anhydrite can be traced across the basin as a positive gamma ray log characteristic. In cores, this marker is a non-calcareous, dark gray fissile shale approximately one inch thick. The first one or two feet of wacke-packstone above this shale often contain intraclasts of fine-grained dolomite and may be slightly argillaceous fine-grained dolomitic mudstones similar to those below the anhydrite units. This occurrence is most frequent in the "B" and "A" sequences.

Overlying the third and uppermost argillaceous marker, another bed of wacke-packstone, variably dolomitized and sometimes slightly argillaceous, comprises the remainder of the upper Red River. The Red River—Stony Mountain contact is marked by a pronounced increase in argillaceous material.

Each of the three sequences is of fairly uniform thickness throughout the basin, but becomes progressively thinner toward their respective depositional limits (pl. 3). The stratigraphically lowest or "C" sequence ranges from 45 to 75 feet thick; the porous zone within it is 25 to 60 feet thick with an average of 30 to 40 feet in the central basin. The thickest "C" porosity zone in North Dakota occurs just east of the basin hinge line, along the eastern edge of the central basin, where the entire "C" sequence consists of porous dolomite capped by a thin anhydrite bed. The "B" depositional sequence ranges from 30 to 70 feet thick and averages around 60 feet thick in the central basin. From the central part of the basin, the "B" sequence thins to the east and eventually coalesces with the overlying "A" sequence. The porous "B" dolomite within the "B" sequence averages only 12 to 14 feet thick. The uppermost, or "A," sequence is 25 to 30 feet thick, with the porous dolomite 2 to 6 feet thick.

The minimum areal distribution of each sequence is approximated by the limits of their respective anhydrite units (fig. 38). The capping anhydrites in each sequence are more laterally restricted than the underlying wackestone and dolomitic mudstone facies. The "A" porosity zone in the uppermost sequence is the least widespread of the three porosity zones, and in North Dakota disappears along a line west of but parallel to the basin hinge line. The wacke-packstone unit above the "A" sequence is approximately 40 feet thick near the basin center, but



Figure 23. Core slab of basal wacke-packstone.
Note wavy organic laminations.

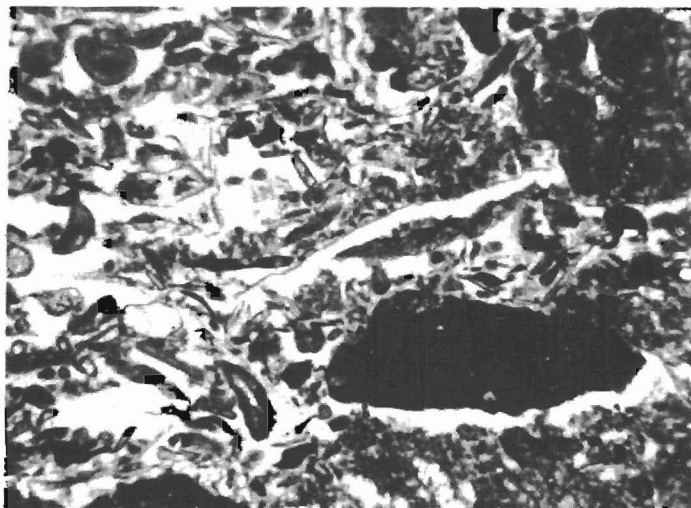


Figure 24. Photomicrograph of intraclastic, skeletal, sparry packstone.
White areas are microspar (plane polarized light).



Figure 25. Core slab of wispy laminated, porous dolomitic mudstone. Note desiccation features along right-hand side.

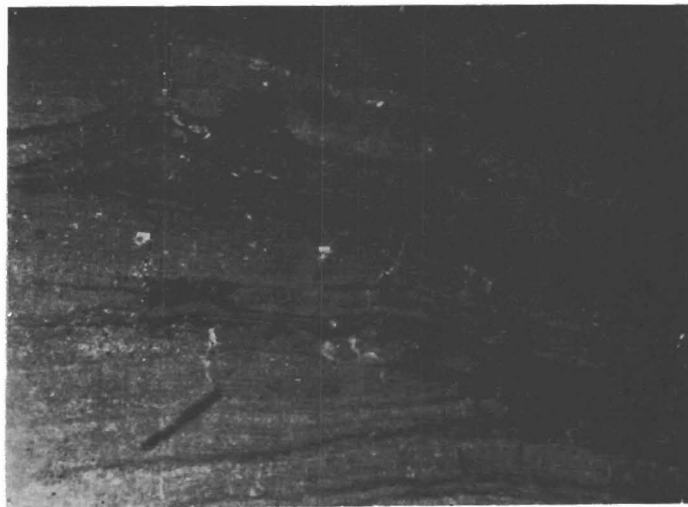


Figure 26. Photomicrograph of desiccation fractures. Rock is greater than 50% dolomite. Note oil stain right of center that follows primary fabric (plane polarized light).

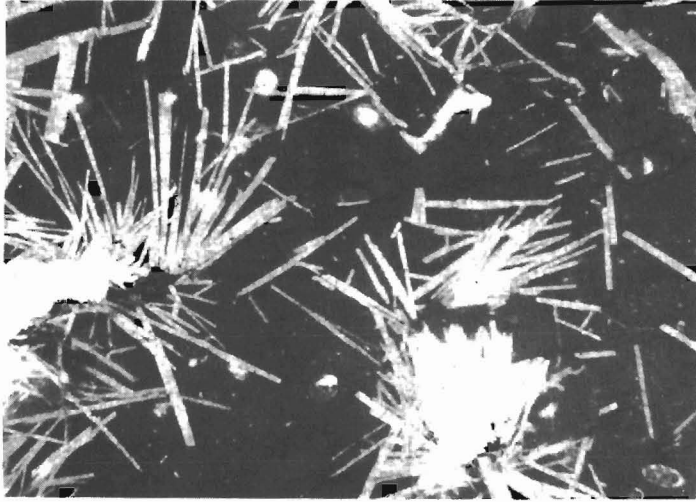


Figure 27. Photomicrograph of acicular anhydrite crystals in dolomitic mudstone (plane polarized light).

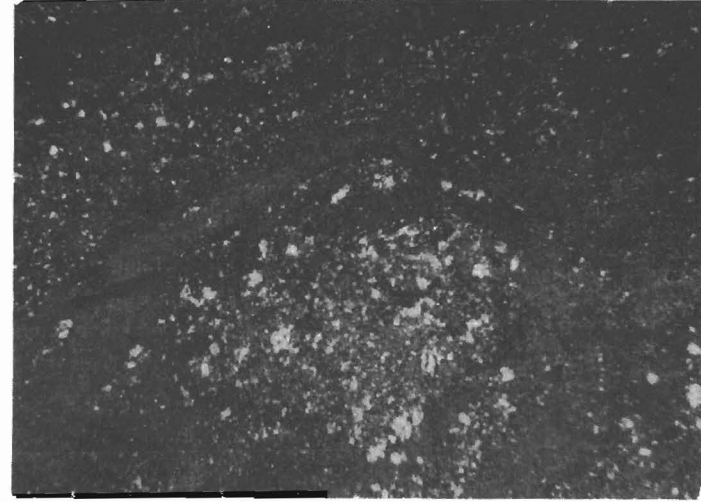


Figure 28. Photomicrograph of subaerial laminated crust in dolomitic mudstone. White areas are voids (plane polarized light).

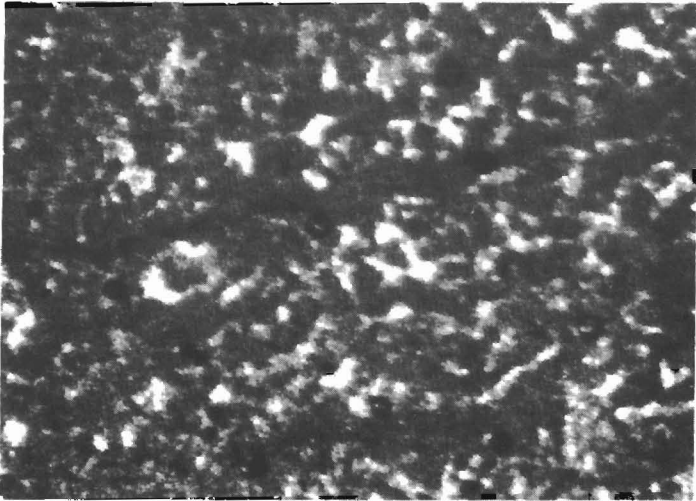


Figure 29. Photomicrograph of pelletal packstone fabric in dolomitic mudstone. Pellets are calcite; clear cement is dolomite (plane polarized light).

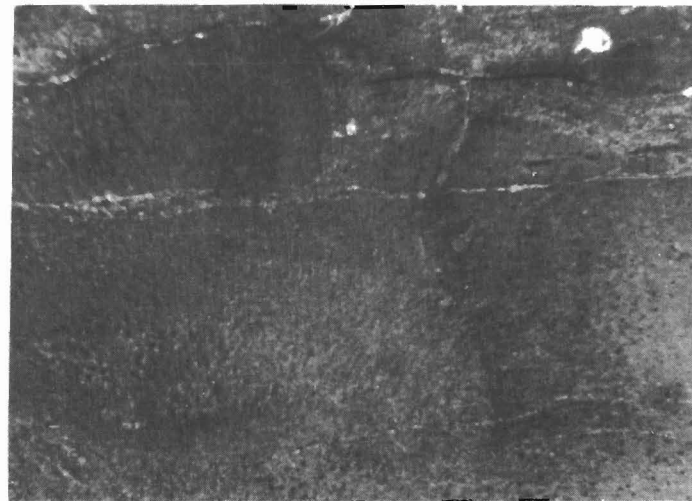


Figure 30. Photomicrograph of cut and fill structure with associated intraclasts in dolomitic mudstone (plane polarized light).



Figure 31. Core slab of undolomitized mudstone.

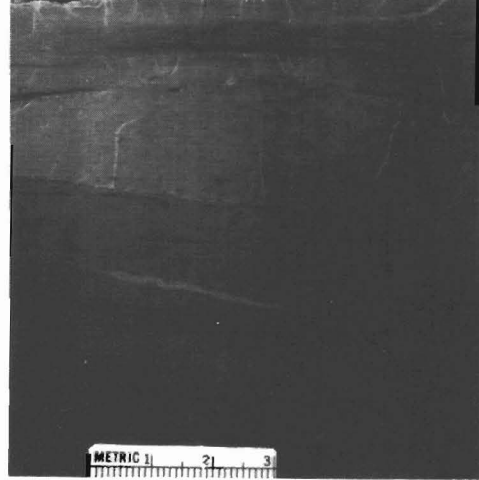


Figure 32. Core slab of thinly bedded dolomitic mudstone.

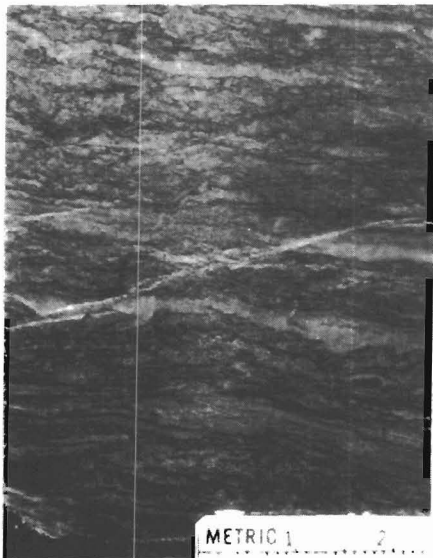


Figure 33. Core slab of possible algal mats in dolomitic mudstone.

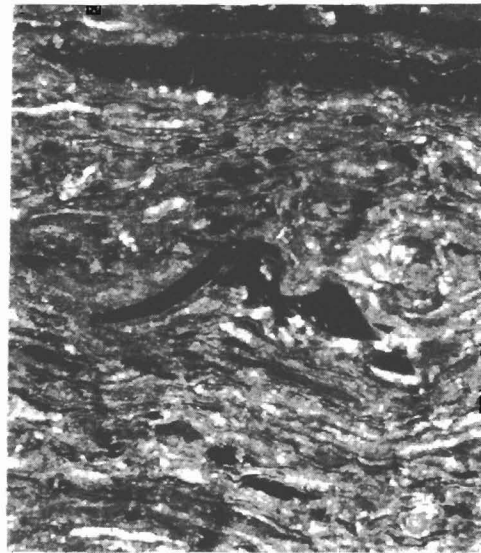


Figure 34. Photomicrograph of possible algal mats in dolomitic mudstone. Most white areas are microspar (plane polarized light).

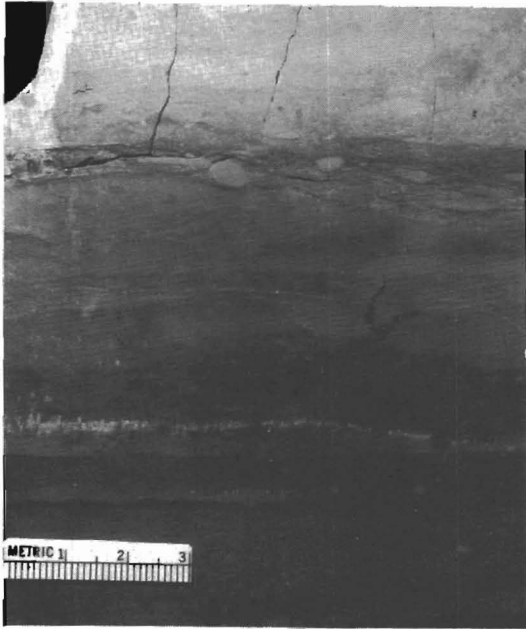


Figure 35. White, very fine-grained, chalky dolomitic mudstone.

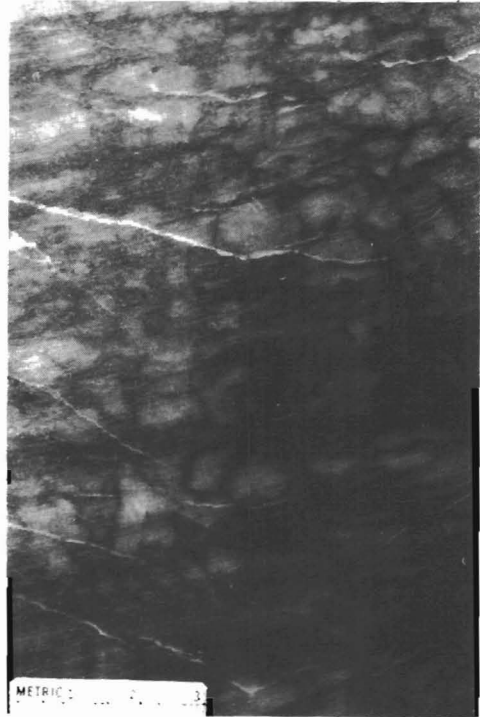


Figure 36. Core slab of nodular anhydrite.

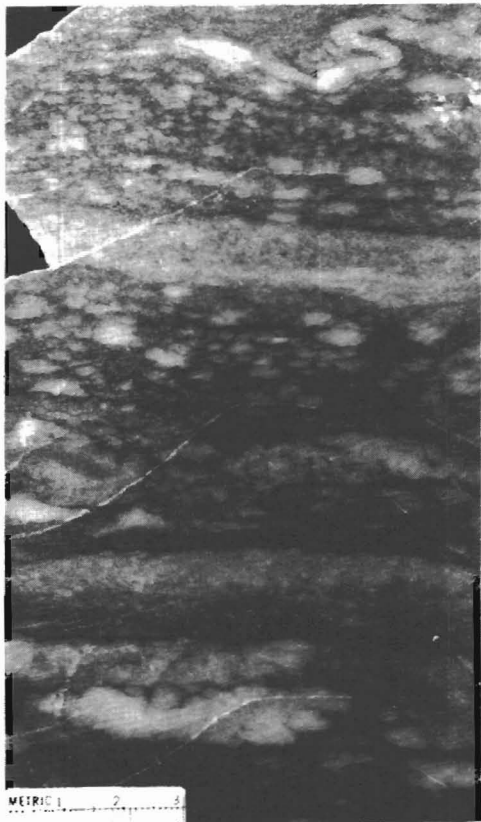


Figure 37. Core slab of nodular anhydrite and thinly bedded anhydrite. Note soft sediment deformation structure at top of photo.

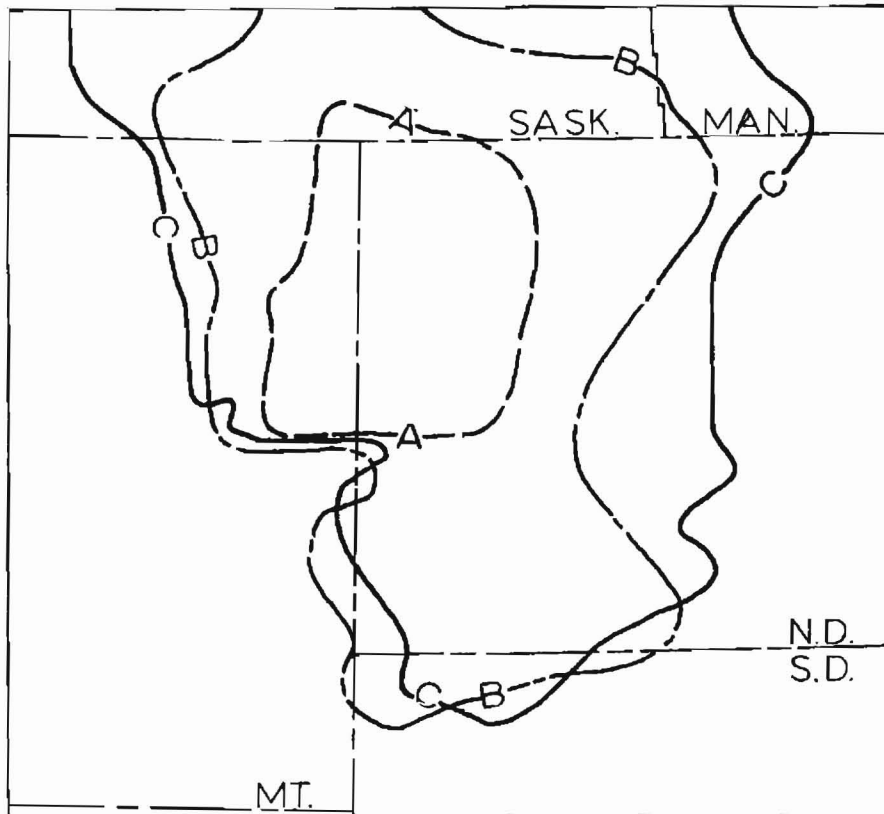


Figure 38. Areal distribution of "C," "B," and "A" anhydrite units (Modified from Mallory, 1972, p. 82).

thins to the east and is non-existent in eastern North Dakota.

Environmental Interpretation

During deposition of each of the three sequences of the upper Red River, the Williston basin was inundated with shallow, normal salinity, open marine water. The basin was bordered by broad intertidal and supratidal flats, probably similar to sabkha environments of the Persian Gulf (Illing, Wells, and Taylor, 1965; Kinsman, 1969), on which evaporitic conditions prevailed. Present day basin slopes are approximately 45 feet per mile on the basin flank and 75 feet per mile in the central basin as determined from structure contours, and paleoslopes are inferred to have been even lower. As the basin filled with sediment, sabkha conditions prograded over the normal marine subtidal environment, and eventually a continuous sheet of supratidal deposits formed to the center of the basin. An areally extensive, very thin layer of argillaceous sediment, superimposed on the sabkha flat sediment, formed during subaerial exposure of the basin. Subsequent reflooding initiated deposition of the following sequence.

The wackestone fabric, general bioturbated character, and normal marine fossil assemblage of the basal unit in each sequence indicates shallow water, open shelf deposition. The sparry packstone fabric near the top of these units probably represents deposition in the low intertidal zone in which tidal action or wave energy winnowed the mud from the coarse skeletal sand. Scattered occurrences of sparry packstone horizons within the wackestone also suggest shallow water and indicate that the sediment substrate was occasionally and repeatedly subjected to high energy conditions. The groups of dark laminations in these strata may be a result of compaction (Shinn et al., 1977).

Several features of the fine-grained dolomite units suggest high intertidal or supratidal deposition. Most indicative are desiccation fractures, acicular anhydrite crystals, and flat pebble breccias. Gastropods, uncommon elsewhere in the section, perhaps also indicate supratidal conditions. Organic-rich laminations in this facies are regarded as poorly preserved algal structures, and pelletal packstones are common. Pelletal fabrics associated with organic-rich algal laminations have been reported as characteristic of supratidal and high intertidal environments (for

example, Illing et al., 1965; Shinn et al., 1965). Fine-grained dolomite may itself be characteristic of the supratidal environment (LaPorte, 1967; Fisher and Rodda, 1969; Goodell and Garman, 1969; Gerhard, 1972; and Milliman, 1974). The chalky white dolomite present in at least three wells represents extreme conditions of subaerial exposure above the supratidal zone, during which fresh water dissolved aragonite and high Mg calcite (Bathurst, 1976; Gerhard et al., 1978).

Nodular anhydrite and the associated inter-laminated anhydrite and dolomite are characteristic sabkha deposits in high supratidal evaporitic environments (Shearman, 1966; Kinsman, 1969).

The argillaceous marker beds, though volumetrically insignificant, are important in that they represent a time of subaerial exposure and non-deposition or erosion. A diastem is inferred from the uniformly thin, widespread character of the markers, as well as the abrupt facies change across them, from high supratidal anhydrite to subtidal wackestone.

Diagenetic Fabrics

Strata of the three depositional sequences show fewer diagenetic steps than the "D" zone. In the subtidal wacke-packstone, diagenetic modification is secondary and not directly related to the depositional environment or the primary fabric. Stylolites proliferate in this facies and some of the grouped, wavy laminations also may be solution features that lack a sutured character. Secondary dolomite rhombs are intimately associated with stylolites and laminations. A large percentage of fossil grains have been either recrystallized or dissolved and filled by microspar and spar, though occasional small vugs probably represent fossil molds that have been enlarged by solution. Crystalline masses of white anhydrite up to one inch across are scattered throughout the wacke-packstone. Notwithstanding these alterations, the primary fabric of wacke-packstone remains essentially intact.

The supratidal sediment was dolomitized penecontemporaneously with deposition. The sediment was initially carbonate mud, probably high Mg calcite and aragonite, as inferred by comparison with mineralogy and texture of sediment in modern analogs (for example, Folk and Land, 1975). The dolomite is not a direct precipitate, as indicated by well-preserved primary fabrics (figs. 25, 26, 31, 32), residual patches of undolomitized micrite, and some

horizons in which the mud was completely unaffected by dolomitization (fig. 30). Dolomitization of the carbonate mud occurred while the sediment was exposed in the supratidal zone, a phenomenon recorded in a number of studies of modern environments (Curtis et al., 1963, Deffeyes et al., 1965; Shinn et al., 1965; and others) and the situation is inferred to be directly analogous to the sabkha environments of the Persian Gulf studied by Illing et al. (1965) and Kinsman (1969). The resulting rocks are considered in this paper to be primary supratidal dolomite. In some cases, micritic pellets form a packstone fabric in which primary dolomite cements the pellets, though the pellets themselves are not dolomitized (fig. 28), a situation similar to that noted by Deffeyes et al. (1965) in supratidal deposits in Bonaire. The pellets probably originated in the intertidal zone (Illing et al., 1965), and may have been carried into the supratidal zone (Shinn et al., 1965).

Limited solution during or slightly after dolomitization resulted in pinpoint porosity with some larger "vugs." The pores only occur where the sediment has been at least partially dolomitized, and are usually surrounded by primary dolomite (fig. 39). Acicular anhydrite and small aggregates of anhydrite frequently precipitated within the dolomitized areas, probably pencontemporaneously with dolomitization.

Minor secondary dolomite in the primary dolomitic mudstone occurs as coarser, clear (limpid) rhombs lining larger vugs (fig. 40). This dolomitization probably occurred much later in the history of the rocks, some time after burial, since a much slower crystallization rate is thought to be necessary to form limpid dolomite (Folk and Land, 1975).

Stylolites are less abundant in the fine-grained dolomite than in the wacke-packstones, but dark brown wispy laminations are common throughout the "A," "B," and "C" porosity zones (figs. 25, 26, 31, 32, 39). Some of these laminations may be secondary solution features, but most appear to be primary, perhaps a result of oxidation during subaerial exposure. No analysis was made of their chemical or mineralogical composition.

The impermeable anhydrite units formed by precipitation of anhydrite within carbonate sediment. The anhydrite formed nodules, which displaced the uncompacted carbonate mud as they grew (Kerr and Thomson, 1963; Shearman, 1966). The anhydrite units are therefore a post-deposi-

tional, pre-lithification phenomenon. Little or no alteration subsequent to their formation is evident, though infrequent small scale loading and flame structures occur, which probably formed during precipitation of the anhydrite (fig. 37). No stylolites or other solution features are seen or expected due to the impermeability of these units, and in any case, evidence of solution would probably be eradicated by subsequent pressure deformation of the anhydrite.

Diagenetic Mechanisms

The diagenetic processes responsible for porosity development in the "A," "B," and "C" zones are more straightforward than those responsible for "D" zone paragenesis (fig. 41). In the upper 3 porosity zones, dolomitization of pre-existing carbonate sediment occurred in the low supratidal zone, seaward of the area of nodular anhydrite precipitation. This dolomitization was a result of interstitial vadose solutions from which anhydrite had precipitated, leaving the solutions with a high Mg/Ca ratio but low overall salinity. Movement of these dolomitizing solutions was caused by evaporative pumping similar to the mechanisms of Newell et al. (1953), Adams and Rhodes (1960), Illing et al. (1965), and Hsu and Siegenthaler (1969), combined with a lateral component of flow induced by evaporation and an oscillating water table controlled by tidal action.

At flood tide, the water table in the supratidal or sabkha flat rose and phreatic marine water was drawn up by evaporative pumping into the vadose zone (fig. 41a). This interstitial water became highly saline due to evaporation, and anhydrite precipitated in the high supratidal area. The lower limit of this anhydrite precipitation was probably the water table or the capillary zone immediately above it (Shearman, 1966; Goodell and Garman, 1969). As the tide ebbed and the water table fell (fig. 41b), evaporation was less effective in drawing water upward from the phreatic zone, and anhydrite precipitation was reduced. It is suggested that the interstitial water remaining in the anhydrite area (high supratidal) was no longer buoyed up by the water table and gravity began to draw it downward, but high evaporation in the lower supratidal zone tended to move it laterally. This movement was in the downdip, seaward direction, which may also have aided movement (Deffeyes et al., 1965). Dolomitization of carbonate mud in the low supratidal area occurred as a result of this influx of inter-

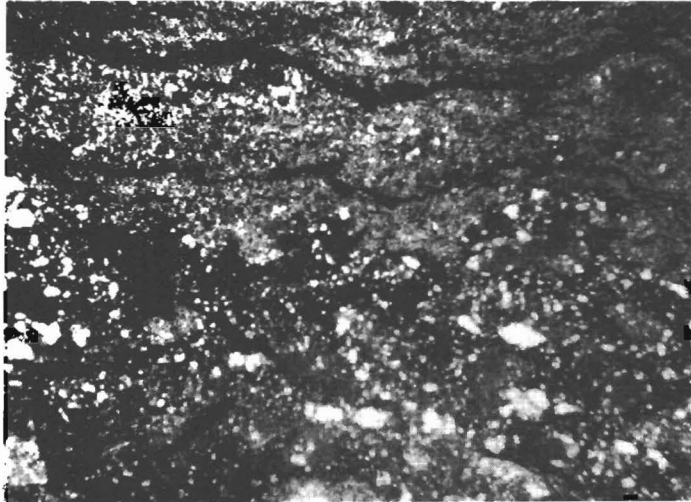


Figure 39. Photomicrograph of pinpoint porosity in dolomitic mudstone. White areas are voids (plane polarized light).

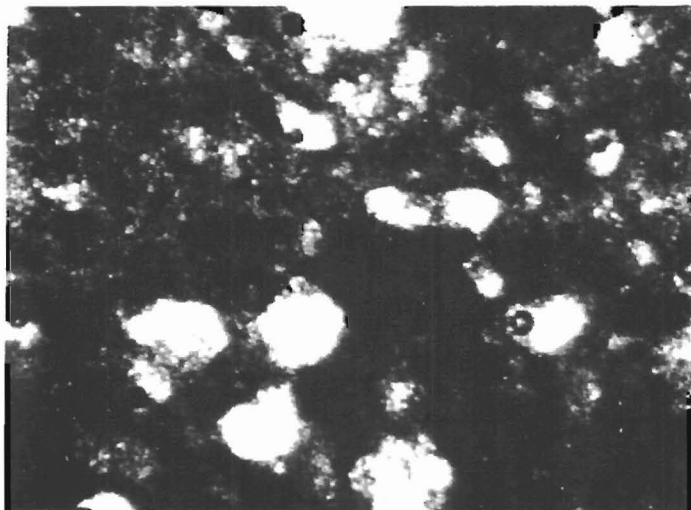


Figure 40. Photomicrograph of secondary dolomite lining vugs in dolomitic mudstone (plane polarized light).

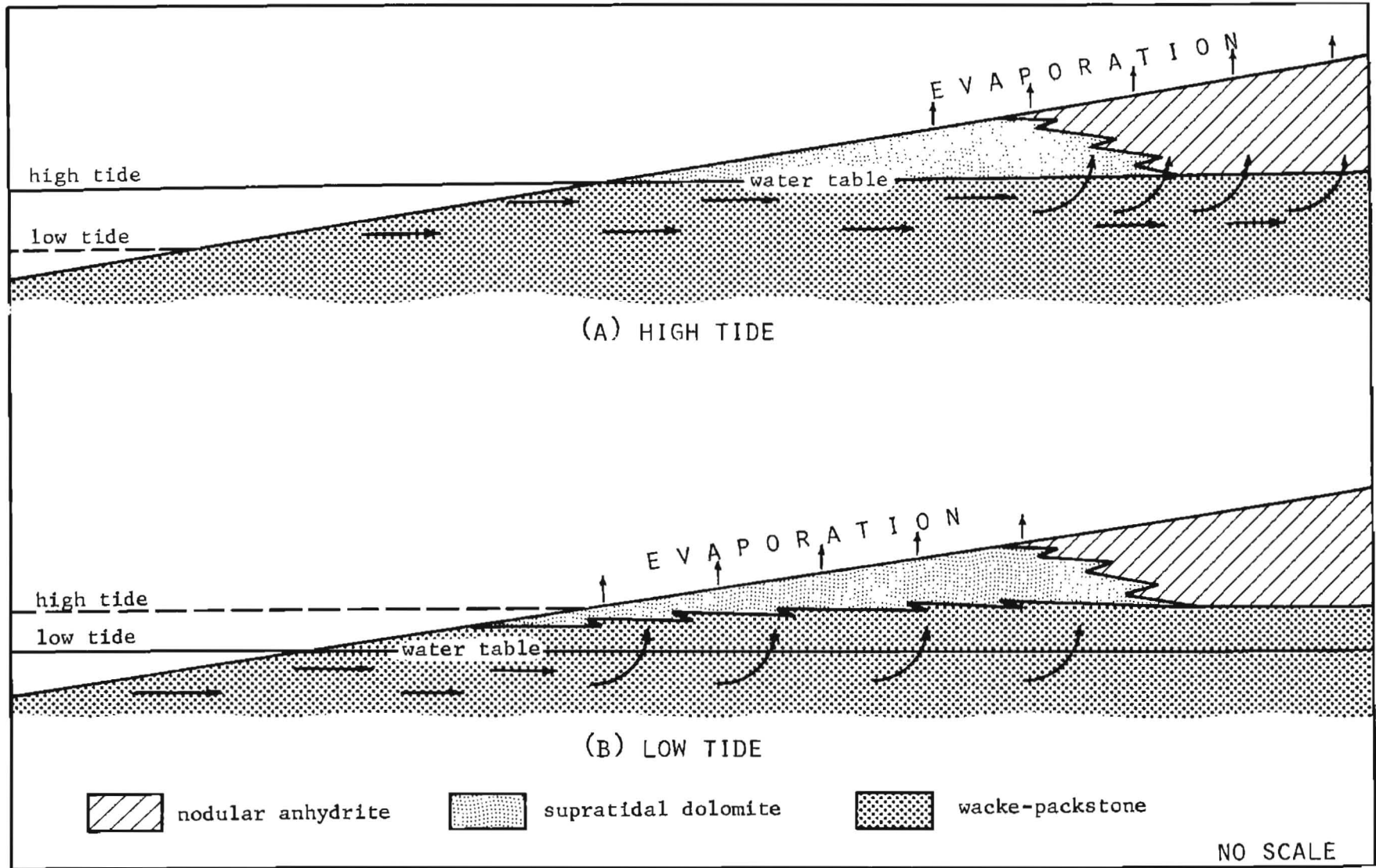


Figure 41. Circulation pattern of dolomitizing solutions in the "A," "B," and "C" porosity zones.

stitial water from which anhydrite had precipitated. Anhydrite precipitation from highly saline water raises the Mg/Ca ratio appreciably by selective removal of calcium, and reduces the overall salinity of the solution. A high Mg/Ca ratio and low overall salinity are ideal dolomitizing conditions (Folk and Land, 1975). In addition to the lateral influx of the interstitial water into the low supratidal zone, water was probably also drawn into the vadose zone from the marine water table by evaporation. The low-tide water table in the low supratidal zone remained close enough to the surface for evaporation to be effective. Mixing of this slightly concentrated saline water from the phreatic zone with high Mg/Ca—low salinity water percolating laterally from the high supratidal area raised the overall salinity of the latter water mass, but the Mg/Ca ratio remained proportionately much larger than if sea water had simply evaporated, and dolomitization probably was not inhibited. The Mg/Ca ratio was rapidly reduced by dolomitization, and intertidal or low intertidal sediment was not often affected.

Successive tides and changes in marine phreatic water table beneath the supratidal environments repeatedly dissolved anhydrite in the low supratidal zone and in the sediment of the high supratidal zone that was below the normal high tide water table. Large quantities of anhydrite probably were not precipitated in the low supratidal zone at high or low tide because normal marine water was continuously drawn from the near surface marine phreatic zone and solutions were not supersaturated with respect to anhydrite. With exception of intermittent storm input, mixing of fresh and marine water masses probably was not an important factor in dolomitization as was the case in the "D" zone.

Microscopic vugs in the primary dolomite probably result from intermittent periods of fresh water influx (Goodell and Garman, 1969) during which the remaining calcite or aragonite mud was dissolved. Secondary dolomitization, which formed crystals that line some of these vugs, probably occurred after the rocks were buried, possibly a result of fresh and marine water mixing during times of subaerial exposure of the basin, as is suggested for second stage dolomitization in the "D" zone.

Porosity Development

Intercrystalline, solution, and fracture porosity characterize the "A," "B," and "C" zones. Best

porosity was produced during primary dolomitization in the depositional environment, during which dolomitization of the carbonate mud on a molecule for molecule basis resulted in intercrystalline porosity (Landes, 1946; Murray, 1960; Weyl, 1960). Additional porosity is due to microscopic solution vugs in the dolomite, and open horizontal fractures of unknown origin that probably occurred much later in the history of the rock. As in the "D" zone, secondary dolomitization did not increase porosity, and may have actually reduced it by partially filling pre-existing vugs and interstices.

DISCUSSION

Deposition of the upper Red River in the Williston basin is shown diagrammatically in figure 42. On the horizontal axis, the basin center is in the middle and the periphery of the basin is at the left and right edges of the diagram. The vertical axis represents time, therefore any horizontal line across the diagram is an isochron. The reader should note that the diagram in no way represents thickness of strata or depth of water in the basin during deposition, but rather shows the lateral changes in lithofacies across the basin at any given time, as well as vertical lithofacies changes at a given location through time. Figure 42 indicates that lateral and vertical facies changes with time in the basin were as follows:

1. Lower Red River sediments were deposited throughout the basin.
2. The lower Red River facies gave way to "D" zone facies, first on the periphery of the basin and later across the entire basin, probably a result of water becoming shallower due to sediment filling the basin. In various areas along the periphery of the basin, shallow barred ponds developed and the organic packstone facies of the "D" zone was deposited.
3. Increasing water depth marked the end of "D" zone deposition, first in the center of the basin and gradually transgressing to include all of the basin proper and part of the basin flank. A minor rise in sea level is sufficient to account for this deepening of the basin, though downwarp of the basin is an alternative explanation. The basal wacke-packstone of the "C" sequence was deposited in the basin at this time, and maximum transgression of the sea is marked by the periphery of this unit. Landward of the periphery of this wacke-packstone, the "C" dolomite rests directly on "D" zone strata.

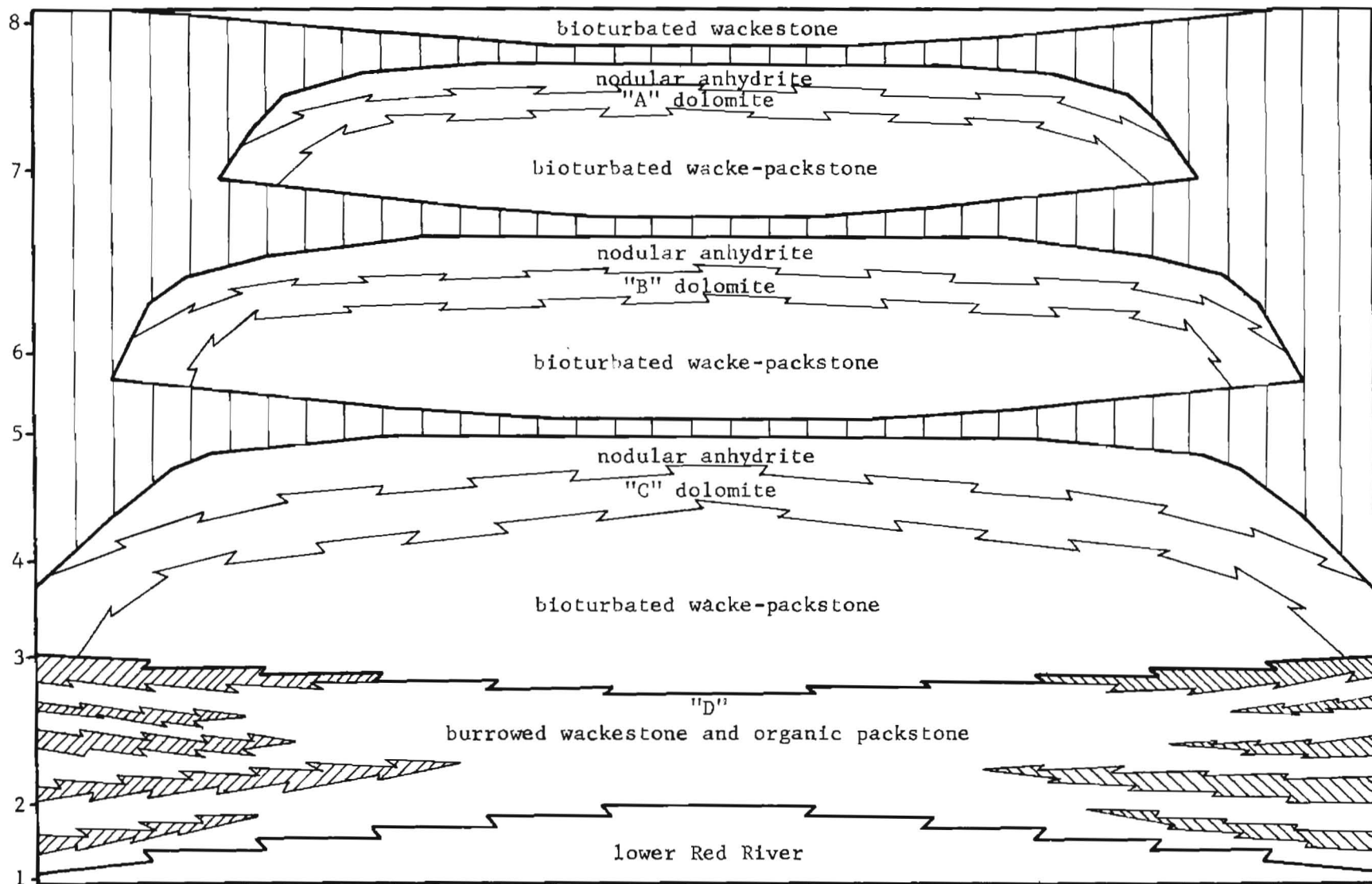


Figure 42. Idealized diagram of upper Red River sedimentation through time.

4. As the basin filled with sediment, the high intertidal to low supratidal dolomite facies, and the high supratidal anhydrite facies began to prograde toward the center of the basin, covering the subtidal wacke-packstone facies.

5. Sabkha conditions eventually prevailed across the entire basin, and supratidal dolomite and anhydrite formed to the center of the basin. A period of essentially non-deposition or erosion followed, during which a very thin layer of fine argillaceous material was deposited.

6. and 7. The basin was flooded twice more during upper Red River deposition, and was subsequently filled with sediment in a manner similar to that described in 3 through 5. Each of these transgressions of the sea was more restricted than the previous one, and the basin was above sea level at the end of each sequence of sedimentation.

8. Following the diastem above the uppermost or "A" sequence, the basin was again flooded and the wacke-packstone at the top of the Red River was deposited.

Porosity in the "A," "B," and "C" zones is directly related to depositional environment. Porosity in these zones is generally poorest in the deepest parts of the basin and best on the flanks due to less subaerial exposure of the basin center to dolomitizing conditions and fresh water solution.

Delineation of paleo-strandlines should be useful in ascertaining where porosity is and is not developed, since deposits in nearshore barred ponds enhance the paragenetic processes responsible for "D" zone porosity, and the porous strata of the "A," "B," and "C" sequences are supratidal sediments. A paleo-strandline can be defined between the "D" zone and the porous dolomite of the "C" sequence, where the subtidal facies (the lowest unit of the "C" sequence) that separates the two zones pinches out to the east and north at the lateral limits of the flooding that followed "D" zone deposition (time 3, fig. 42). The point at which the two zones can no longer be separated is a strandline, that is, the position at which the sediment overlying the "D" zone changes facies from subtidal wackestone to supratidal dolomite. This paleo-strandline represents maximum transgression of the sea at this time (pl. 4). Two lines are plotted on this map, one indicating where the "C" and "D" zones definitely can be separated, the second where they cannot. Logs in the area between the lines cannot be picked with cer-

tainty, and the area may be thought of loosely as an intertidal zone. The strandline follows isopach contours closely, even around the embayment in Wells County. Major divergence from this pattern occurs just north of the embayment, at which point the strandline crosses isopachs as it continues around the north side of the basin. This may result from higher sedimentation rates in this area, or less compaction of the sediment through time, though a reason for either possibility is not apparent. Data in this area are sparse and no investigation of this apparent anomaly was attempted. On the Nesson anticline the strandline returns to the same isopach as on the east side of the basin.

With sufficient core data, a second and third strandline could be located where the subtidal deposits of the "B" and "A" sequences change facies to supratidal sediments, and thus the geometry of the basin during each successive flooding could be determined. These later strandlines occur between the "B" dolomite and "C" anhydrite, and between the "A" dolomite and "B" anhydrite. Given the thin character of all the units of the upper two sequences in the areas where the strandlines are expected, and the variability of porosity and lack of core, it has not been possible to locate the later strandlines with any certainty.

The Nesson anticline was clearly a feature of some topographic expression during upper Red River sedimentation. Units thin as they cross it, more shallow pond (organic) deposits are present in the "D" zone than in the center of the basin, and thicker "A," "B," and "C" porosity zones occur indicating more supratidal exposure. The paleo-strandline follows isopachs around the anticline (pl. 4), indicating the anticline was, if not subaerially exposed, at least a prominent high at the time.

The small structural highs referred to in various parts of this paper are also of interest, since porosity in these areas should be well-developed if the features were topographic highs during deposition. For example, in the Shell 34X-31-1 well in the Mondak field in McKenzie County, the upper Red River section is structurally higher than in other wells in the area and at least four organic units are present in the "D" zone, while other wells near the center of the basin consist predominantly of the burrowed facies. Porosity in the "D" zone in this well is well-developed. Whereas 34X-31-1 is not eco-

nomical to produce, Shell's Swigart well approximately a half mile to the west in Montana is higher on the same structure and does produce. Therefore, "D" zone porosity has developed in the center of the basin if the proper conditions existed during deposition.

The combination of topographic highs during deposition and activity of the same structures through time has resulted in adequate porosity and structural closure to form structural-stratigraphic hydrocarbon traps. Depositional thins and present structural highs can be correlated on isopach and structure contour maps in Bowman County due to good well control, and some correlation is possible in other parts of the basin, notably McKenzie County. At present, structural control of paleo-topographic features in the basin as a result of recurring activity of basement structures can only be suggested. A comprehensive study locating formational thins through the section, combined with structure contour mapping would do much to prove or disprove this hypothesis.

HYDROCARBON PRODUCTION AND POTENTIAL

Past and Current Production

Red River oil in North Dakota was first discovered in Williams County in 1957 with Amerada Petroleum Company's Iverson-Nelson Unit 1 in the Beaver Lodge Field. Subsequent Red River discoveries, all in the western part of the state, now produce throughout the entire north-south length of the state. Exploration of the Red River and subsequent production has greatly accelerated in the last ten years. In 1965, fifty-four Red River producers in four fields accounted for 3.3 percent of North Dakota's total oil production. By 1970 Red River production had increased to 6.1 percent of the state's total. In 1975, one hundred six Red River wells in nineteen fields produced 9.2 percent of North Dakota's oil, or 1,878,841 barrels of 20,452,498 total barrels produced in North Dakota in that year (N.D.G.S., 1965, 1970, 1975).

The largest amount of Red River production is currently from Bowman and Williams Counties. Most production in Bowman County is from the Cedar Creek Field in the western part of the county. Of five other fields in Bowman County, the largest is the Medicine Pole Hills Field. Most fields in this county are associated with small structural highs. In the northern part of the state

in Williams County most Red River production is from the Beaver Lodge and Tioga Fields, both of which lie on the Nesson anticline. Additional production in this area occurs in smaller fields surrounding these two. Between the two north and south major producing areas are not less than eight recognized fields and a substantial number of additional producers in unnamed fields. Scattered production occurs in Divide, McKenzie, Dunn, Billings, Slope, and Stark Counties, with the largest amount in McKenzie County. The Buffalo Creek Field in Stark County represents the easternmost Red River production in the state. Production in the above counties in which no major structures are recognized stems from small seismic highs and facies changes that are often associated with the highs. Substantial new production from several wells in Dunn County is from what appears to be a sizable structural high or number of highs (North Dakota Industrial Commission Order 1544).

Six porosity zones labeled "A" to "F" downhole occur in the Red River. The "E" and "F" zones are in the lower Red River and most tests are not drilled to them. The "E" zone does not produce oil anywhere in North Dakota, and only one well, the Amerada B-1 Ives in the Tioga Field, produces from the "F" zone. A recent test in McKenzie County may also produce from the "F" horizon. The "A" through "D" zones all produce in North Dakota; however, various porosity zones are more productive in some parts of the state than in others. Production from the "A" zone occurs largely on the Cedar Creek anticline, while "B," "C," and "D" production is scattered throughout the state (Friestad, 1969).

Oil accumulation in the Red River occurs in both structural and stratigraphic traps. The Beaver Lodge and Tioga Fields on the Nesson anticline are examples of major structural traps in North Dakota. Other smaller structural highs, combined with the associated porosity development discussed previously, are responsible for production in McKenzie, Dunn, Bowman and other counties.

Potential for Production

The Billings nose and the structure in the Hettinger-Stark-Morton County area are excellent prospects for further hydrocarbon exploration. Thinning of upper Red River strata in these areas indicates depositional highs which have been shown to favorably affect porosity develop-

ment. The location of these structures in the main part of the basin where the upper Red River stratigraphic succession is fully developed is also favorable.

The small highs in Burleigh and Emmons Counties, particularly the western flanks of these structures, warrant careful investigation. The two "D" zone facies should be well-developed in this area, though the potential of the upper three zones in this area may be limited by lateral termination of the anhydrite cap rocks.

The embayment in Wells County provides a particularly interesting situation. While the basinal character itself is not conducive to oil entrapment, the stratigraphic succession of the main basin is developed here, and any small structures associated with this feature should be examined carefully.

Very little is known of the basin hinge line or structures associated with it north of the Wells embayment. Also, the main basin between the hinge line and Dunn County has very few test wells drilled to the Red River, therefore it is difficult to evaluate the hydrocarbon potential of the area at this time. New production from the center of the basin in Dunn County indicates that this area from the center of the basin eastward is worthy of investigation as well.

CONCLUSIONS

1. Depositional environments, each with a characteristic lithofacies, were constant across most of the basin in North Dakota, resulting in laterally continuous units with uniform primary fabrics. Therefore, while primary fabric is important to subsequent diagenetic processes, lateral changes in the depositional environments themselves cannot be called upon to explain variable porosity within a given rock unit.

2. Diagenetic changes in the primary rock fabric are responsible for most of the porosity in all four zones. Porosity in the "A," "B," and "C" zones is due to dolomitization that was penecontemporaneous with deposition of the primary carbonate sediment. Porosity in the "D" zone also stems from syndepositional dolomitization of sediment in the burrows, as well as later calcite solution. Most porosity in these zones is therefore a result of intercrystalline voids in syndepositional (primary) dolomite.

3. The dolomitic mudstones and nodular anhydrite units of the "C," "B," and "A" sequences of the upper Red River are directly

analogous to the sabkha environments of the Persian Gulf, studied by Illing et al. (1965) and Kinsman (1969). No modern analog is known for the "D" zone.

4. Dolomitization in all four porosity zones can be attributed to high Mg/Ca ratios, reduced salinity, and interstitial movement of dolomitizing fluids.

5. Small differences in primary permeability within a body of sediment are often sufficient to affect syndepositional diagenesis, which may in turn have a direct effect on porosity development. For example, preferential syndepositional dolomitization of burrows over matrix in the "D" zone has resulted in much greater porosity in the burrows, and preferential primary dolomitization of matrix over pellets in some horizons of the upper three porosity zones has affected porosity in these horizons.

6. Structural or topographic highs in the basin during upper Red River deposition resulted in thinning of the Red River strata and, perhaps more importantly, affected syndepositional diagenetic processes. In the "D" zone, depositional highs caused solutions to flow around rather than over the highs, resulting in less dolomitization and less porosity on top of the highs. After burial of the strata, the structural highs adversely affected calcite solution and the associated porosity development, again by channeling solutions around the highs. Topographic highs may have favorably affected porosity development in the "A," "B," and "C" zones by exposing sediment to dolomitization in the supratidal zone, which resulted in intercrystalline porosity. During this exposure, intermittent fresh water flushing developed microscopic vugs.

7. In light of 6, exploration of the "D" zone should be concentrated "around" rather than "on" structures, and "A," "B," and "C" exploration should be concentrated "on" structure.

8. Several large areas in North Dakota show good potential for further expansion of hydrocarbon production in the upper Red River.

REFERENCES CITED

- Adams, J. E., and Rhodes, M. L., 1960, Dolomitization by seepage reflexion: American Association of Petroleum Geologists Bulletin, v. 44, p. 1912-1920.
- Andrichuk, J. M., 1959, Ordovician and Silurian stratigraphy and sedimentation in southern Manitoba, Canada: American Association of Petroleum Geologists Bulletin, v. 43, p. 2333-2398.
- Radiozamani, K., 1973, The Dorag dolomitization model-application to the Middle Ordovician of Wisconsin: Journal of Sedimentary Petrology, v. 43, p. 965-984.
- Baillie, A. D., 1952, Ordovician geology of the Lake Winnipeg and adjacent areas, Manitoba: Manitoba Mines Branch Publication 51-6, 64 p.
- Ballard, F. V., 1963, Structural and stratigraphic relationships in the upper Paleozoic rocks of eastern North Dakota: North Dakota Geological Survey Bulletin 40, 42 p.
- Bassler, R. S., 1915, Bibliographic index of American Ordovician and Silurian fossils: U.S. Natural Museum Bulletin 92, 1521 p.
- Bathurst, R. G. C., 1976, Carbonate sediments and their diagenesis: Elsevier, New York, 658 p.
- Carlson, C. G., and Anderson, S. B., 1965, Sedimentary and tectonic history of North Dakota part of Williston basin: American Association of Petroleum Geologists Bulletin, v. 49, p. 1833-1846.
- Curtis, R., Evans, G., Kinsman, D. J. J., and Shearman, D. J., 1963, Association of dolomite and anhydrite in the Recent sediments of the Persian Gulf: Nature, v. 197, p. 679-680.
- Deffeyes, K. S., Lucia, F. J., and Weyl, P. K., 1965, Dolomitization of Recent and Plio-Pleistocene sediments by marine evaporite waters on Bonaire, Netherlands Antilles, in L. C. Pray and R. C. Munay, eds., Dolomitization and limestone diagenesis: Society of Economic Paleontologists and Mineralogists Special Publication 13, p. 71-88.
- Dowling, D. B., 1900, Report on the geology of the west shore and islands of Lake Winnipeg: Geological Survey of Canada Annual Report, Part F, 100 p.
- Dunham, R. J., 1962, Classification of carbonate rocks according to depositional texture, in W. E. Ham, ed., Classification of carbonate rocks: American Association of Petroleum Geologists, Memoir 1, p. 108-121.
- Fisher, W. L., and Rodda, P. V., 1969, Edward Formation (Lower Cretaceous), Texas: dolomitization in a carbonate platform system: American Association of Petroleum Geologists Bulletin, v. 53, p. 55-72.
- Flower, R. H., 1952, New Ordovician cephalopods from eastern North America: Journal of Paleontology, v. 26, p. 24-59.
- Foerste, A. F., 1928, American arctic and related cephalopods: Denison University Bulletin, Scientific Laboratory Journal, v. 23, p. 1-110.
- Foerste, A. F., 1929, The cephalopods of the Red River Formation of southern Manitoba: Denison University Bulletin, Scientific Laboratory Journal, v. 24, p. 129-235.
- Folk, R. L., and Land, L. S., 1975, Mg/Ca ratios and salinity: two controls over crystallization of dolomite: American Association of Petroleum Geologists Bulletin, v. 59, p. 60-68.
- Friestad, H. K., 1969, The Upper Red River Formation (Ordovician) in western North Dakota: Master's thesis, University of North Dakota, Grand Forks, 82 p.
- Fuller, J. G. C. M., 1961, Ordovician and continuous formations in North Dakota: American Association of Petroleum Geologists Bulletin, v. 45, p. 1334-1363.
- Gebelein, C. D., and Hoffman, P., 1973, Algal origin of dolomite laminations in stromatolitic limestones: Journal of Sedimentary Petrology, v. 43, p. 603-613.
- Gerhard, L. C., 1972, Canadian depositional environments and paleotectonics, central Colorado: in Quarterly of the Colorado School of Mines, v. 67, p. 1-36.
- Gerhard, L. C., Frost, S. H., and Curth, P. J., 1978, Stratigraphy and depositional setting, Kingshill limestone, Miocene, St. Croix, U.S. Virgin Islands: American Association of Petroleum Geologists Bulletin, v. 62, p. 403-418.
- Goodell, H. G., and Garman, R. K., 1969, Carbonate geochemistry of Superior deep test well, Andros Island, Bahamas: American Association of Petroleum Geologists Bulletin, v. 53, p. 513-536.

- Hanshaw, B. B., Back, W., and Deike, R. C., 1971, A geochemical hypothesis for dolomitization by ground water: *Economic Geology*, v. 66, p. 710-724.
- Horodyski, R. J., and Vonder Haar, S. P., 1975, Recent calcareous stromatolites from Laguna Mormona (Baja California) Mexico: *Journal of Sedimentary Petrology*, v. 45, p. 894-906.
- Horodyski, R. J., Bloeser, B., and Vonder Haar, S. P., 1977, Laminated algal mats from a coastal lagoon, Laguna Mormona, Baja California, Mexico: *Journal of Sedimentary Petrology*, v. 47, p. 680-696.
- Hsu, K. J., and Siegenthaler, C., 1969, Preliminary experiments on hydrodynamics movement induced by evaporation and their bearing on the dolomite problem: *Sedimentology*, v. 12, p. 11-25.
- Hussey, R. C., 1926, The Richmond Formation of Michigan: University of Michigan Contributions Museum Geology, v. 2, p. 113-187.
- Illing, L. V., Wells, A. J., and Taylor, J. C. M., 1965, Penecontemporary dolomite in the Persian Gulf: in L. C. Pray and R. C. Murray, eds., *Dolomitization and limestone diagenesis*: Society of Economic Paleontologists and Mineralogists Special Publication 13, p. 89-111.
- Irwin, M. L., 1965, General theory of epeiric clear water sedimentation: *American Association of Petroleum Geologists Bulletin*, v. 49, p. 445-459.
- Kay, G. M., 1935, Ordovician Stewartville Dubuque problems: *Journal of Geology*, v. 43, p. 561-690.
- Kendall, A. C., 1974, The hydrocarbon potential of the Bighorn Group (Ordovician) in southern Saskatchewan, in G. R. Parslow, ed., *Fuels: a geological appraisal*: Saskatchewan Geological Society Special Publication 2, p. 125-148.
- Kerr, S. D., Jr., and Thomson, A., 1963, Origin of nodular and bedded anhydrite in Permian shelf sediments, Texas and New Mexico: *American Association of Petroleum Geologists Bulletin*, v. 47, p. 1726-1732.
- Kinsman, D. J. J., 1969, Modes of formation, sedimentary associations, and diagnostic features of shallow-water and supratidal evaporites: *American Association of Petroleum Geologists Bulletin*, v. 53, p. 830-840.
- Landes, K. K., 1946, Porosity through dolomitization: *American Association of Petroleum Geologists Bulletin*, v. 30, p. 305-318.
- LaPorte, L. F., 1967, Carbonate deposition near mean sea-level and resultant facies mosaic: Manlius Formation (Lower Devonian) of New York state: *American Association of Petroleum Geologists Bulletin*, v. 51, p. 73-101.
- Macauley, G., and Leith, E. I., 1951, Winnipeg Formation of Manitoba (abst.) *Geological Society of America Bulletin*, v. 62, p. 1461-1462.
- Mallory, W. W., ed., 1972, *Geologic atlas of the Rocky Mountain region*: Rocky Mountain Association of Geologists, Denver, Colorado, p. 77.
- Milliman, J. D., 1974, *Marine carbonates*: Springer-Verlag, New York, 375 p.
- Murray, R. C., 1960, Origin of porosity in carbonate rocks: *Journal of Sedimentary Petrology*, v. 30, p. 59-84.
- Newell, N. D., Rigby, J. K., Fischer, A. G., Whiteman, A. J., Hickox, J. E., and Bradley, J. S., 1953, The Permian reef complex of the Guadalupe Mountains region, Texas and New Mexico—a study in paleoecology: W. H. Freeman Co., San Francisco, 236 p.
- North Dakota Geological Survey, 1965, Production statistics and engineering data, oil in North Dakota, first half 1965.
—1966, Production statistics and engineering data, oil in North Dakota, second half 1965.
—1971, Production statistics and engineering data, oil in North Dakota, first half 1970.
—1971, Production statistics and engineering data, oil in North Dakota, second half 1970.
—1976, Production statistics and engineering data, oil in North Dakota, first half 1975.
—1976, Production statistics and engineering data, oil in North Dakota, second half 1975.
- Porter, J. W., and Fuller, J. G. C. M., 1959, Lower Paleozoic rocks of northern Williston basin and adjacent areas: *American Association of Petroleum Geologists Bulletin*, v. 43, p. 124-189.
- Ross, R. J., Jr., 1957, Ordovician fossils from wells in the Williston basin, eastern Montana: U.S. Geological Survey Bulletin 1021, Pt. M, p. 439-510.
- Sandberg, C. A., 1964, Precambrian to Mississippian Paleotectonics of the southern Williston basin: 3rd International Williston Basin Symposium, p. 37-38.

- Shearman, D. J., 1966, Origin of marine evaporites by diagenesis: Institute of Mining and Metallurgy Transactions, v. 75, p. 208-215.
- Shinn, E. A., Ginsburg, R. N., and Lloyd, R. M., 1965, Recent supratidal dolomite from Andros Island, Bahamas, *in* L. C. Pray and R. C. Murray, eds., Dolomitization and limestone diagenesis: Society of Economic Paleontologists and Mineralogists Special Publication 13, p. 112-123.
- Shinn, E. A., Halley, R. B., Hudson, J. H., and Lidy, B. H., 1977, Limestone compaction: an enigma: *Geology*, v. 5, p. 21-24.
- Sinclair, G. W., 1959, Succession of Ordovician rocks in southern Manitoba: Geological Survey of Canada Paper 59-5, 9 p.
- Twenhofel, W. H., chmn., 1954, Correlation of Ordovician formations of North America: Geological Society of America Bulletin, v. 65, p. 247-298.
- Weyl, P. K., 1960, Porosity through dolomitization: conservation-of-mass requirements: *Journal of Sedimentary Petrology*, v. 30, p. 85-90.
- Whiteaves, J. F., 1897, The fossils of the Galena-Trenton and Black River Formations of Lake Winnipeg and its vicinity: Geological Survey of Canada, Paleozoic Fossils, v. 3, Pt. 3, p. 129-242.

APPENDIX A WELL LOCATION INDEX

ADAMS COUNTY

Amerada Hess Corp. NDGS No. 6050	Holmquist No. 1 SW $\frac{1}{4}$ sec 30, T129N, R98W
-------------------------------------	---

BENSON COUNTY

Calvert Exploration Co. NDGS No. 632	A. J. & I. John & G. Stadum No. 1 NW $\frac{1}{4}$ SE $\frac{1}{4}$ sec 31, T154N, R70W
---	--

BILLINGS COUNTY

Amerada Petr. Corp. NDGS No. 291	H. May No. 1 NW $\frac{1}{4}$ NE $\frac{1}{4}$ sec 9, T139N, R100W
Stanolind Oil and Gas Co. NDGS No. 555	N.W.I. (N.P.) No. 1 SE $\frac{1}{4}$ SE $\frac{1}{4}$ sec 17, T143N, R100W
Shell-Northern Pacific Railway Co. NDGS No. 2853	Gov't No. 41X-5-1 NE $\frac{1}{4}$ NE $\frac{1}{4}$ sec 5, T143N, R101W
Amerada Petr. Corp. NDGS No. 3268	Scoria No. 8 NE $\frac{1}{4}$ SW $\frac{1}{4}$ sec 10, T139N, R101W
Davis Oil Co. NDGS No. 3746	Kevin Fed No. 1 SW $\frac{1}{4}$ SW $\frac{1}{4}$ sec 10, T138N, R100W
Pan Am. Petr. Corp. NDGS No. 4254	USA A. G. Macauey "B" No. 1 SE $\frac{1}{4}$ NW $\frac{1}{4}$ sec 28, T137N, R100W
Lone Star Prod. Co. NDGS No. 5195	A. Schwartz "B" No. 1 SE $\frac{1}{4}$ NE $\frac{1}{4}$ sec 2, T137N, R100W
Tenneco Oil Co. NDGS No. 6169	Burlington Northern No. 1 NW $\frac{1}{4}$ NW $\frac{1}{4}$ sec 25, T143N, R101W
Tenneco Oil Co. NDGS No. 6303	Burlington Northern No. 1-29 NE $\frac{1}{4}$ SW $\frac{1}{4}$ sec 29, T143N, R100W

BOTTINEAU COUNTY

California Oil Co. NDGS No. 38	Blanche Thomson No. 1 SW $\frac{1}{4}$ SE $\frac{1}{4}$ sec 31, T160N, R81W
Lion Oil Co. NDGS No. 286	Erickson No. 1 SW $\frac{1}{4}$ NE $\frac{1}{4}$ sec 32, T164N, R78W
Amerada Petr. Corp. NDGS No. 4655	H. D. Lillestrand No. 1 SE $\frac{1}{4}$ SW $\frac{1}{4}$ sec 31, T162N, R78W

BOWMAN COUNTY

W. H. Hunt-Z. Brooks NDGS No. 485	State No. 1 NW $\frac{1}{4}$ NW $\frac{1}{4}$ sec 16, T129N, R104W
Western Natural Gas Co. NDGS No. 516	Truax-Traer Coal No. 1 NW $\frac{1}{4}$ SW $\frac{1}{4}$ sec 13, T132N, R102W
J. H. Snowden et al. NDGS No. 1446	M. A. Morrison #1 SE $\frac{1}{4}$ SW $\frac{1}{4}$ sec 34, T130N, R103W
Carter Oil Co. NDGS No. 1575	L. & E. Johnson No. 1 NW $\frac{1}{4}$ SW $\frac{1}{4}$ sec 9, T129N, R106W
Shell Oil Co. NDGS No. 2509	Gov't. No. 41-23A NE $\frac{1}{4}$ NE $\frac{1}{4}$ sec 23, T130N, R107W
Shell Oil Co. NDGS No. 2677	Gov't No. 34X-3A-2 SW $\frac{1}{4}$ SE $\frac{1}{4}$ sec 3, T130N, R107W
H. W. Clarkson & E. W. Clarkson NDGS No. 3150	Clarkson-White et al. #1 NE $\frac{1}{4}$ SE $\frac{1}{4}$ sec 27, T130N, R107W
Continental Oil Co. NDGS No. 3261	Fed. No. 1 NW $\frac{1}{4}$ NE $\frac{1}{4}$ sec 15, T129N, R106W
Houston Oil and Minerals NDGS No. 3312	R. Young No. 33-4 NW $\frac{1}{4}$ SE $\frac{1}{4}$ sec 4, T129N, R106W
Shell Oil Co. NDGS No. 3514	Gov't. No. 43-30C-43 NE $\frac{1}{4}$ SE $\frac{1}{4}$ sec 30, T130N, R106W
Shell Oil Co. NDGS No. 3720	Gov't. No. 31X-34B-45 NW $\frac{1}{4}$ NE $\frac{1}{4}$ sec 34, T131N, R107W
Shell Oil Co. NDGS No. 3798	Gov't. No. 13-32 NW $\frac{1}{4}$ SW $\frac{1}{4}$ sec 32, T131N, R106W
A. H. Hodges Ind., Inc. NDGS No. 4143	C. Hestekin No. 1 NE $\frac{1}{4}$ NE $\frac{1}{4}$ sec 15, T130N, R104W

Farm. Union Centr. Exch., Inc. NDGS No. 4158	F. A. Carlson No. 31-8 NW $\frac{1}{4}$ NE $\frac{1}{4}$ sec 8, T129N, R106W
Farm. Union Centr. Exch., Inc. NDGS No. 4248	Gov't. No. 11-5 NW $\frac{1}{4}$ NW $\frac{1}{4}$ sec 5, T129N, R106W
A. J. Hodges Ind., Inc. NDGS No. 4538	Susas-Wick No. 1-X NE $\frac{1}{4}$ SW $\frac{1}{4}$ sec 15, T130N, R104W
Pel-Tex Petr. Co., Inc. NDGS No. 4545	J. C. Kennedy NW $\frac{1}{4}$ NE $\frac{1}{4}$ sec 17, T130N, R100W
Golden Eagle Exploration, Ltd. NDGS No. 4577	C. Holecek No. 1 NE $\frac{1}{4}$ NE $\frac{1}{4}$ sec 17, T129N, R104W
Ashland Oil and Refining Co. NDGS No. 4641	A. L. Fossum No. 1 NE $\frac{1}{4}$ NW $\frac{1}{4}$ sec 22, T130N, R104W
International Nuclear Corp. NDGS No. 4654	J. M. Susa et al. No. 1-61 SW $\frac{1}{4}$ NE $\frac{1}{4}$ sec 30, T130N, R102W
Superior Oil Co. NDGS No. 4662	Holecek No. 1 SE $\frac{1}{4}$ SE $\frac{1}{4}$ sec 8, T129N, R104W
International Nuclear Corp. NDGS No. 4669	Miller No. 1-62 SW $\frac{1}{4}$ NE $\frac{1}{4}$ sec 21, T131N, R104W
Calvert Drilling and Producing Co. NDGS No. 4756	C. Holecek No. 17-4 NW $\frac{1}{4}$ SE $\frac{1}{4}$ sec 17, T129N, R104W
Amarillo Oil Co. NDGS No. 4821	N.D. State No. 1-16 NE $\frac{1}{4}$ NE $\frac{1}{4}$ sec 16, T130N, R104W
Amarillo Oil Co. NDGS No. 4832	A. Fossum No. 1-24 S $\frac{1}{2}$ NW $\frac{1}{4}$ sec 24, T130N, R104W
Calvert Drilling and Producing Co., et al. NDGS No. 4841	Holecek-Olson No. 18-4 SE $\frac{1}{4}$ SE $\frac{1}{4}$ sec 19, T129N, R104W
Pel-Tex, Inc. NDGS No. 4922	I. & N. Landa No. 1 SE $\frac{1}{4}$ SW $\frac{1}{4}$ sec 5, T130N, R100W
Amarillo Oil Co. NDGS No. 4932	E. Fossum No. 1-24 NW $\frac{1}{4}$ NE $\frac{1}{4}$ sec 24, T130N, R104W
Pel-Tex, Inc. NDGS No. 4952	G. R. Boor, et al. No. 1 SW $\frac{1}{4}$ SW $\frac{1}{4}$ sec 32, T130N, R100W
Amarillo Oil Co. NDGS No. 4954	A. Fossum No. 2-13 NW $\frac{1}{4}$ NW $\frac{1}{4}$ sec 13, T130N, R104W
Pel-Tex, Inc. NDGS No. 5000	E. Coates et al. No. 1 SW $\frac{1}{4}$ SW $\frac{1}{4}$ sec 28, T131N, R105W
Amarillo Oil Co. NDGS No. 5045	Nelson No. 1-14 C NE $\frac{1}{4}$ sec 14, T130N, R104W
Amarillo Oil Co. NDGS No. 5061	E. Fossum No. 2-13 C SE $\frac{1}{4}$ sec 13, T130N, R104W
Pennzoil United, Inc. NDGS No. 5070	Swanke No. 1 NW $\frac{1}{4}$ NW $\frac{1}{4}$ sec 15, T131N, R105W
Amarillo Oil Co. NDGS No. 5089	A. Fossum No. 3-23 C E $\frac{1}{4}$ SE $\frac{1}{4}$ sec 23, T130N, R104W
Pel-Tex, Inc. NDGS No. 5128	F. N. Stricherz No. 1 SW $\frac{1}{4}$ NE $\frac{1}{4}$ sec 30, T130N, R104W
Amarillo Oil Co. NDGS No. 5133	Anderson No. 1-12 C W $\frac{1}{2}$ NW $\frac{1}{4}$ sec 12, T130N, R104W
Farmers Union Central Exchange, Inc. NDGS No. 5163	N.D. No. 15X-16 C S $\frac{1}{2}$ S $\frac{1}{2}$ sec 16, T131N, R104W
Eason Oil Co. NDGS No. 5200	C. Olson No. 1-13 SE $\frac{1}{4}$ NW $\frac{1}{4}$ NW $\frac{1}{4}$ sec 13, T129N, R105W
Depco, Inc. NDGS No. 5209	Dronen No. 33-20 NW $\frac{1}{4}$ SE $\frac{1}{4}$ sec 20, T130N, R103W
Depco, Inc. NDGS No. 5227	Greni No. 33-26 NW $\frac{1}{4}$ SE $\frac{1}{4}$ sec 26, T129N, R103W
Farmers Union Central Exchange, Inc. NDGS No. 5256	H. and T. Gete No. 1 SE $\frac{1}{4}$ SW $\frac{1}{4}$ sec 22, T131N, R104W
Depco, Inc. NDGS No. 5262	Greni No. 22-26 SE $\frac{1}{4}$ NW $\frac{1}{4}$ sec 26, T129N, R103W

Rainbow Resources, Inc.
NDGS No. 5266

Farmers Union Central
Exchange, Inc.
NDGS No. 5269

Depco, Inc.
NDGS No. 5270

Rainbow Resources, Inc.
NDGS No. 5278

Depco, Inc.
NDGS No. 5347

Eason Oil Co.
NDGS No. 5382

Farmers Union Central
Exchange, Inc.
NDGS No. 5397

K. Luff & Hanover Planning
NDGS No. 5402

K. Luff & Hanover Planning
NDGS No. 5403

Rainbow Resources, Inc.
NDGS No. 5421

Rainbow Resources, Inc.
NDGS No. 5456

Depco, Inc.
NDGS No. 5459

Eason Oil Co.
NDGS No. 5492

Patrick Petr. Corp.
NDGS No. 5495

Amax Petr. Corp.
NDGS No. 5567

K. Luff & Hanover Planning
NDGS No. 5584

K. Luff
NDGS No. 5618

Depco, Inc.
NDGS No. 5651

Petroleum, Inc.
NDGS No. 5700

K. Luff
NDGS No. 5712

Pennzoil Co.
NDGS No. 5733

Farmers Union Central
Exchange, Inc.
NDGS No. 5745

True Oil Co.
NDGS No. 5772

K. Luff & Hanover Planning, Inc.
NDGS No. 5823

Farmland International
NDGS No. 5829

Depco, Inc.
NDGS No. 5865

Farmland International
NDGS No. 5882

Farmland International
NDGS No. 5892

K. Luff & Rainbow Resources, Inc.
NDGS No. 5895

Petroleum, Inc.
NDGS No. 5904

A. Fossum No. 2-14
SE $\frac{1}{4}$ SW $\frac{1}{4}$ sec 14, T130N, R104W

R. M. Miller No. 7X-27

C N $\frac{1}{2}$ sec 27, T131N, R104W

Hughes No. 13-27
NW $\frac{1}{4}$ SW $\frac{1}{4}$ sec 27, T129N, R103W

Oakland BND No. 1-2
SW $\frac{1}{4}$ SW $\frac{1}{4}$ sec 2, T130N, R104W

Homquist No. 31-8
NW $\frac{1}{4}$ NE $\frac{1}{4}$ sec 8, T131N, R104W

Jorgenson No. 21-44X
S $\frac{1}{2}$ SE $\frac{1}{4}$ sec 21, T129N, R104W

M. Miller No. 4-21

NW $\frac{1}{4}$ NW $\frac{1}{4}$ sec 21, T131N, R104W

Jett No. 1-28
NE $\frac{1}{4}$ NW $\frac{1}{4}$ sec 28, T124N, R101W

Hughes No. 1-27
SE $\frac{1}{4}$ NW $\frac{1}{4}$ sec 27, T129N, R103W

C. Hesterin No. 2A
SW $\frac{1}{4}$ NE $\frac{1}{4}$ sec 15, T130N, R104W

Wallman No. 1-8
NE $\frac{1}{4}$ SW $\frac{1}{4}$ sec 8, T130N, R104W

Peters No. 14-29
SW $\frac{1}{4}$ SW $\frac{1}{4}$ sec 29, T130N, R102W

Olson No. 18-34X
SW $\frac{1}{4}$ SE $\frac{1}{4}$ sec 18, T129N, R104W

Mann-Grem No. 1
SE $\frac{1}{4}$ NE $\frac{1}{4}$ sec 4, T129N, R103W

N.D. State No. 1
SW $\frac{1}{4}$ SE $\frac{1}{4}$ sec 36, T129N, R106W

Paris et al. No. 1-22
SE $\frac{1}{4}$ SW $\frac{1}{4}$ sec 22, T130N, R102W

G. Hughes No. 1-15
C S $\frac{1}{2}$ N $\frac{1}{2}$ sec 15, T129N, R103W

Nygaard No. 44-30
SE $\frac{1}{4}$ SE $\frac{1}{4}$ sec 30, T130N, R103W

Arithson No. 1
SE $\frac{1}{4}$ SW $\frac{1}{4}$ sec 34, T129N, R104W

Richards No. 1-28
C E $\frac{1}{2}$ sec 28, T130N, R102W

Bagley No. 1
NE $\frac{1}{4}$ SW $\frac{1}{4}$ sec 11, T129N, R102W

Miller No. 6-23

SE $\frac{1}{4}$ NW $\frac{1}{4}$ sec 23, T131N, R104W

Fisher No. 11-5
C NW $\frac{1}{4}$ NW $\frac{1}{4}$ sec 5, T131N, R100W

Mosbrucker No. 1-8
NE $\frac{1}{4}$ SE $\frac{1}{4}$ sec 6, T130N, R102W

Oakland Wick No. 1-11
C SW $\frac{1}{4}$ NW $\frac{1}{4}$ sec 11, T130N,
R104W

Fleming No. 14-32
C SW $\frac{1}{4}$ SW $\frac{1}{4}$ sec 32, T130N, R102W

Arithson-Fed. No. 1-35
SE $\frac{1}{4}$ SE $\frac{1}{4}$ sec 35, T129N, R104W

Oakland-Nelson No. 2-11
SE $\frac{1}{4}$ SE $\frac{1}{4}$ sec 11, T130N, R104W

State No. 1-16
C N $\frac{1}{2}$ N $\frac{1}{2}$ sec 16, T130N, R102W

Hilton No. 1
C NW $\frac{1}{4}$ NE $\frac{1}{4}$ sec 34, T131N, R103W

K. Luff & Pennzoil Co.
NDGS No. 5709

K. Luff
NDGS No. 5920

K. Luff
NDGS No. 5951

Petroleum, Inc. et al.
NDGS No. 5967

Farmland International et al.
NDGS No. 6074

F. Paulson No. 1-24
C W $\frac{1}{2}$ NW $\frac{1}{4}$ sec 24, T130N, R102W

M. L. Peters No. 1-20
NW $\frac{1}{4}$ NE $\frac{1}{4}$ sec 20, T130N, R102W

W. Anderson No. 1-3
SW $\frac{1}{4}$ NE $\frac{1}{4}$ sec 3, T130N, R103W

Arithson No. 1-D
NE $\frac{1}{4}$ NW $\frac{1}{4}$ sec 34, T129N, R104W

Richards & Southland Royalty
No. 1-2
C SE $\frac{1}{4}$ SE $\frac{1}{4}$ sec 2, T129N, R102W

BURLEIGH COUNTY

Continental Oil Co.
NDGS No. 155

Continental Oil Co.
NDGS No. 174

C. Hunt Trust Estate
NDGS No. 701

C. Hunt Trust Estate
NDGS No. 723

C. Hunt Trust Estate
NDGS No. 756

C. Hunt Trust Estate
NDGS No. 763

C. Hunt Trust Estate
NDGS No. 765

C. Hunt Trust Estate
NDGS No. 772

Dronen No. 1
NE $\frac{1}{4}$ NE $\frac{1}{4}$ sec 9, T140N, R75W

Dueneland No. 1
NW $\frac{1}{4}$ NW $\frac{1}{4}$ sec 3, T140N, R77W

Board of Univ. and School Lands #1
NE $\frac{1}{4}$ NE $\frac{1}{4}$ sec 36, T144N, R75W

R. P. Schlabach No. 1
NE $\frac{1}{4}$ NE $\frac{1}{4}$ sec 36, T139N, R76W

R. A. Nicholson No. 1
SE $\frac{1}{4}$ SE $\frac{1}{4}$ sec 32, T137N, R77W

A. Nory No. 1
SE $\frac{1}{4}$ SE $\frac{1}{4}$ sec 14, T144N, R77W

Soder Investment Co. No. 1
SW $\frac{1}{4}$ SW $\frac{1}{4}$ sec 31, T142N, R76W

P. Rybert No. 1
NW $\frac{1}{4}$ NW $\frac{1}{4}$ sec 23, T140N, R79W

DIVIDE COUNTY

Kerr McGee Oil Ind., Inc.
NDGS No. 1546

Carter Oil Co.
NDGS No. 2010

Miami Oil Producers, Inc. et al.
NDGS No. 4837

H. L. Hunt
NDGS No. 5192

Oil Development Co. of Texas
NDGS No. 5248

A. Johnson No. 1
NE $\frac{1}{4}$ NW $\frac{1}{4}$ sec 34, T162N, R101W

D. D. Moore No. 1
NW $\frac{1}{4}$ NE $\frac{1}{4}$ sec 7, T163N, R102W

R. Hagen No. 1
SW $\frac{1}{4}$ NE $\frac{1}{4}$ sec 12, T160N, R100W

A. B. Erickson No. 1
SW $\frac{1}{4}$ NE $\frac{1}{4}$ NE $\frac{1}{4}$ sec 3, T160N,
R95W

Rogers No. 1
NE $\frac{1}{4}$ NE $\frac{1}{4}$ sec 10, T160N, R98W

DUNN COUNTY

Socony-Vacuum Oil Co., Inc.
NDGS No. 505

Socony-Vacuum Oil Co.
NDGS No. 793

Amerada Petr. Corp.
NDGS No. 3044

Sinclair Oil and Gas Co.
NDGS No. 4220

Hemerich & Payne, Inc.
NDGS No. 4611

Kathol Petr., Inc.-
Noble Drilling Corp.
NDGS No. 4725

Miami Oil Producers, Inc.
NDGS No. 4957

Mesa Petr. Co.
NDGS No. 5621

Alpar Resources Inc.
NDGS No. 5887

Amoco Production Co.
NDGS No. 5971

C. Dvorak No. 1
SE $\frac{1}{4}$ NE $\frac{1}{4}$ sec 6, T141N, R94W

Solomon Bird Bear et al.
No. F-22-22-1
SE $\frac{1}{4}$ NW $\frac{1}{4}$ sec 22, T149N, R91W

M. Selle T-1 No. 1
NE $\frac{1}{4}$ NE $\frac{1}{4}$ sec 27, T143N, R92W

N. A. Knudsvig No. 1
SW $\frac{1}{4}$ NE $\frac{1}{4}$ sec 13, T145N, R94W

N.D. State No. 1
SW $\frac{1}{4}$ SW $\frac{1}{4}$ sec 36, T146N, R96W

Little Mo No. 1-24
SW $\frac{1}{4}$ SE $\frac{1}{4}$ sec 24, T148N, R97W

Estate of H. Robe No. 1
NW $\frac{1}{4}$ NW $\frac{1}{4}$ sec 8, T147N, R93W

Roshav No. 1
NE $\frac{1}{4}$ NW $\frac{1}{4}$ sec 23, T142N, R97W

McNamara No. 1
SW $\frac{1}{4}$ SW $\frac{1}{4}$ sec 8, T144N, R92W

G. Carlson No. 1
C NE $\frac{1}{4}$ NW $\frac{1}{4}$ sec 6, T145N, R94W

Amoco Production Co.
NDGS No. 6086

B. Selle No. 1
CNE $\frac{1}{4}$ NE $\frac{1}{4}$ sec 7, T146N, R94W

EMMONS COUNTY

Northern Ordinance
NDGS No. 18

Franklin Investment Co. No. 1
C NW $\frac{1}{4}$ NW $\frac{1}{4}$ sec 35, T133N, R75W

Roeser-Pendleton
NDGS No. 23

J. J. Weber No. 1
SE $\frac{1}{4}$ sec 35, T133N, R78W

Peak Drilling Co.
NDGS No. 43

Ohlhauser No. 1
NE $\frac{1}{4}$ SE $\frac{1}{4}$ sec 8, T132N, R78W

FOSTER COUNTY

Frazier-Conroy Drilling Co.
NDGS No. 287

S. Dunbar No. 1
NW $\frac{1}{4}$ NW $\frac{1}{4}$ sec 13, T146N, R63W

Pure Oil Co.
NDGS No. 403

J. M. Carr No. 1
NE $\frac{1}{4}$ NE $\frac{1}{4}$ sec 15, T146N, R66W

GOLDEN VALLEY COUNTY

Guif Oil Corp.
NDGS No. 410

Dorough Fed. No. 1
NE $\frac{1}{4}$ SW $\frac{1}{4}$ sec 24, T143N, R103W

Amerada Petr. Corp.
NDGS No. 4130

R. Waldron No. 1
SW $\frac{1}{4}$ NW $\frac{1}{4}$ sec 9, T138N, R105W

Texas Gas Expl. Corp.
NDGS No. 5438

G. M. Brown et al. No. 1
NE $\frac{1}{4}$ NW $\frac{1}{4}$ sec 27, T141N, R105W

GRANT COUNTY

Cardinal-Lone Star-National
Bulk Carriers, Inc.
NDGS No. 3636

M. Bierwagen No. 1

SW $\frac{1}{4}$ NE $\frac{1}{4}$ sec 1, T133N, R90W

Helmerich & Payne, Inc.
NDGS No. 5097

Burlington Northern "J" No. 27-1
NE $\frac{1}{4}$ NW $\frac{1}{4}$ sec 27, T131N, R88W

Helmerich & Payne, Inc.
NDGS No. 5118

Burlington Northern "L" No. 23-1
NE $\frac{1}{4}$ SW $\frac{1}{4}$ sec 23, T130N, R88W

Wainoco, Inc.
NDGS No. 5496

Krause No. 22-5
SE $\frac{1}{4}$ NW $\frac{1}{4}$ sec 5, T134N, R90W

HETTINGER COUNTY

Socony-Vacuum Oil Co., Inc.
NDGS No. 611

C. & M. Jacobs F14-24P
SW $\frac{1}{4}$ SW $\frac{1}{4}$ sec 24, T134N, R96W

Pubeo Petr. Corp.
NDGS No. 4984

J. Haberstroh No. 12-2
NW $\frac{1}{4}$ NE $\frac{1}{4}$ sec 12, T135N, R92W

W. H. Hunt
NDGS No. 5447

V. Senn No. 1
C SE $\frac{1}{4}$ SW $\frac{1}{4}$ sec 15, T136N, R92W

KIDDER COUNTY

Magnolia Petr. Co.
NDGS No. 24

Dakota "A" Strat. Test
NE $\frac{1}{4}$ sec 36, T141N, R73W

Carter Oil Co.
NDGS No. 230

N.D. State No. 1
NE $\frac{1}{4}$ SE $\frac{1}{4}$ sec 16, T143N, R71W

C. Hunt Trust Estate
NDGS No. 748

E. B. Sauter No. 1
NW $\frac{1}{4}$ NE $\frac{1}{4}$ sec 32, T142N, R74W

LOGAN COUNTY

C. Hunt Trust Estate
NDGS No. 590

F. M. Fuller No. 1
SW $\frac{1}{4}$ SE $\frac{1}{4}$ sec 6, T136N, R73W

Wise Oil Co. No. 2 et al.
NDGS No. 5523

B. A. Weigel No. 1
NW $\frac{1}{4}$ NW $\frac{1}{4}$ sec 29, T135N, R78W

McHENRY COUNTY

Hunt Oil Co.
NDGS No. 39
Hunt Oil Co.
NDGS No. 61

W. B. Shoemaker No. 1
NE $\frac{1}{4}$ SW $\frac{1}{4}$ sec 3, T157N, R78W
P. Lennertz No. 1
NW $\frac{1}{4}$ SE $\frac{1}{4}$ sec 17, T153N, R77W

McKENZIE COUNTY

Gulf Oil Corp.
NDGS No. 956
Amerada Petr. Corp.
NDGS No. 2373

Bennie Pierre Fed. No. 1
NW $\frac{1}{4}$ SW $\frac{1}{4}$ sec 28, T148N, R104W
Antelope "A" No. 1
NW $\frac{1}{4}$ NE $\frac{1}{4}$ SE $\frac{1}{4}$ sec 1, T152 N,
R95W

Shell Oil Co.-Northern
Pacific Railway
NDGS No. 2584

Texaco, Inc.
NDGS No. 2602

Quintana Petroleum Corp.
NDGS No. 3645

Tiger Oil Co.
NDGS No. 3804

Shell Oil Co.
NDGS No. 4062

Helmerich & Payne, Inc.

NDGS No. 4305

Consolidated Oil & Gas, Inc. &
Miami Oil

NDGS No. 4723

Consolidated Oil & Gas, Inc.-
Miami Oil

NDGS No. 4807

General American Oil Co. of Texas
NDGS No. 5002

Pennzoil Co.
NDGS No. 5655

Shell Oil Co.
NDGS No. 5821

Tiger Oil Co.
NDGS No. 5840

State 32-16-1

SW $\frac{1}{4}$ NE $\frac{1}{4}$ sec 16, T145N, R101W

S. A. Garlaad No. 5
NE $\frac{1}{4}$ sec 6, T153N, R95W

U.S.A. No. 1
SE $\frac{1}{4}$ SE $\frac{1}{4}$ sec 24, T145N, R105W

R. Slaaten, No. 1
NW $\frac{1}{4}$ SW $\frac{1}{4}$ sec 23, T153N, R95W

22X-28-1
NW $\frac{1}{4}$ SE $\frac{1}{4}$ NW $\frac{1}{4}$ sec 28, T148N,
R101W

Fed. McKenzie No. 1

(OWDD-AFE-7607)

NE $\frac{1}{4}$ NW $\frac{1}{4}$ sec 33, T146N, R104W

Fed. Land Bank No. 1

SE $\frac{1}{4}$ NE $\frac{1}{4}$ sec 23, T151N, R101W

Fed. Land Bank No. 24-1

NW $\frac{1}{4}$ sec 24, T151N, R101W

Burlington Northern No. 1-9
SE $\frac{1}{4}$ NW $\frac{1}{4}$ sec 9, T146N, R103W

Fed. No. 25-1
C SW $\frac{1}{4}$ sec 25, T150N, R104W

Gov't. No. 34X-31-1
SW $\frac{1}{4}$ SE $\frac{1}{4}$ sec 31, T149N, R104W

Fed. No. 26-1
NE $\frac{1}{4}$ SE $\frac{1}{4}$ sec 28, T150N, R104W

McLEAN COUNTY

Stanolind Oil & Gas Co.
NDGS No. 49

McLean Co. No. 1
SW $\frac{1}{4}$ SW $\frac{1}{4}$ sec 28, T150N, R80W

MERCER COUNTY

F. F. Kelly
NDGS No. 21

F. Leutz No. 1
NW $\frac{1}{4}$ NE $\frac{1}{4}$ sec 28, T142N, R89W

MORTON COUNTY

Pan Am. Petr. Corp.
NDGS No. 1620

R. Yetter No. 1
NE $\frac{1}{4}$ SW $\frac{1}{4}$ sec 27, T139N, R90W

Amerada Petr. Corp.
NDGS No. 3859

J. Meyer No. 1
SE $\frac{1}{4}$ NE $\frac{1}{4}$ sec 34, T135N, R83W

Austral Oil Co. Inc.
NDGS No. 3978

J. J. Leingang 6524 No. 1
SE $\frac{1}{4}$ NW $\frac{1}{4}$ sec 34, T137N, R83W

Campbell & Partners
NDGS No. 5379

Picha No. 1
C NW $\frac{1}{4}$ NE $\frac{1}{4}$ sec 5, T138N, R83W

MOUNTRAIL COUNTY

Empire State Oil Co. et al.
NDGS No. 4386

Vorwerk No. 1
SE $\frac{1}{4}$ SE $\frac{1}{4}$ sec 28, T151N, R90W

Amerada Hess Corp.
NDGS No. 5072

A. Erickson No. 2X
NE $\frac{1}{4}$ NE $\frac{1}{4}$ sec 22, T158N, R94W

OLIVER COUNTY

Carter Oil Co.
NDGS No. 15

E. L. Semling No. 1
C SE $\frac{1}{4}$ sec 18, T141N, R81W

Youngblood & Youngblood
NDGS No. 95

E. Wachter No. 1
SE $\frac{1}{4}$ SW $\frac{1}{4}$ sec 3, T141N, R81W

General American Oil Co. of Texas
NDGS No. 4940

R. Henke No. 1-24
SE $\frac{1}{4}$ SW $\frac{1}{4}$ sec 24, T142N, R85W

PIERCE COUNTY

Midwest Exploration Co.
NDGS No. 435

Heckman No. 1
SW $\frac{1}{4}$ NE $\frac{1}{4}$ sec 12, T158N, R69W

Shell Oil Co.
NDGS No. 706

G. Marchus No. 1
SE $\frac{1}{4}$ SE $\frac{1}{4}$ sec 23, T157N, R70W

A. J. Hodges Ind., Inc.
NDGS No. 3920

A. Martin No. 1
SE $\frac{1}{4}$ SE $\frac{1}{4}$ sec 23, T152N, R74W

ROLETTE COUNTY

T. M. Evans Production Corp.
NDGS No. 316

A. J. Johnson No. 1
NW 1/4 SW 1/4 sec 23, T160N, R70W

SHERIDAN COUNTY

Caroline Hunt Trust Estate
NDGS No. 665

C. Hunt Trust Estate
NDGS No. 684

C. Hunt Trust Estate
NDGS No. 693

C. Hunt Trust Estate
NDGS No. 735

J. Waltz, Sr. No. 1
NE 1/4 NE 1/4 sec 15, T148N, R76W

J. R. Matz No. 1
NE 1/4 NE 1/4 sec 1, T147N, R75W

W. E. Bauer No. 1
SW 1/4 SW 1/4 sec 19, T146N, R76W

C. A. Pfeiffer No. 1
SW 1/4 SW 1/4 sec 16, T146N, R74W

SIOUX COUNTY

Ohio Oil Co.
NDGS No. 631

Standing Rock Sioux Tribal No. 1
NE 1/4 SW 1/4 sec 29, T131N, R60W

SLOPE COUNTY

Deep Rock Stanolind
NDGS No. 91

Pan Am. Petr. Corp.
NDGS No. 3363

Sun Oil Co.
NDGS No. 3588

H. L. Hunt
NDGS No. 4075

H. L. Hunt
NDGS No. 4124

H. L. Hunt
NDGS No. 4241

Amerada Petr. Corp.
NDGS No. 4280

States Oil Co.
NDGS No. 4749

Belco Petr. Corp.
NDGS No. 5210

J. Chambers
NDGS No. 5933

J. Brusich No. 1
SE 1/4 SE 1/4 sec 8, T135N, R98W

L. Foreman No. 1
SW 1/4 SE 1/4 sec 23, T133N, R106W

Greer Fed. No. 1
SE 1/4 SE 1/4 sec 21, T134N, R105W

NPRR "A" No. 1
NE 1/4 SW 1/4 sec 9, T136N, R101W

E. Hayden No. 1
NW 1/4 SE 1/4 sec 4, T136N, R101W

NPRR "A" No. 3
NE 1/4 NW 1/4 sec 23, T136N, R101W

I. Mitchell No. 1
NE 1/4 SW 1/4 sec 18, T135N, R103W

J. J. Sedevie No. 1
SW 1/4 NW 1/4 sec 33, T133N, R101W

Cannonball No. 3-3
NE 1/4 NW 1/4 sec 3, T133N, R100W

H. J. Burke No. 1
SE 1/4 SW 1/4 sec 9, T133N, R102W

STARK COUNTY

W. H. Hunt
NDGS No. 850

Continental Oil Co.
NDGS No. 3515

Texaco, Inc.
NDGS No. 4134

Texaco, Inc.
NDGS No. 4182

Union Oil Co. of Calif.
NDGS No. 4311

Bridger Petr. Corp.
NDGS No. 5142

Lofe Star Producing Co.
NDGS No. 5143

Continental Oil Co.
NDGS No. 5255

A. Privratsky No. 1
NW 1/4 NW 1/4 sec 15, T138N, R98W

C. Sloxen No. 1
NW 1/4 NW 1/4 sec 9, T140N, R93W

A. Schrank (NCT-1) No. 1
NW 1/4 SE 1/4 sec 15, T137N, R92W

A. Schrank (NCT-1) No. 2
C SW 1/4 sec 23, T137N, R92W

V. H. Kudrna No. 1
NE 1/4 SW 1/4 sec 20, T139N, R97W

B. Kilzer No. 1
SE 1/4 NE 1/4 sec 9, T137N, R92W

Wanner No. 1
NE 1/4 NW 1/4 sec 9, T137N, R97W

Feimer-Anger No. 1
NE 1/4 SW 1/4 sec 22, T137N, R95W

STUTSMAN COUNTY

Barnet Drilling Inc.
NDGS No. 40

General Atlas Carbon Co.
NDGS No. 134

Calvert Exploration Co.
NDGS No. 668

Calvert Exploration Co.
NDGS No. 669

John Gaier No. 1
NW 1/4 NW 1/4 sec 11, T141N, R67W

F. Borthel No. 1
SW 1/4 NE 1/4 sec 15, T142N, R65W

M. Meyers No. 1
SE 1/4 SW 1/4 sec 25, T137N, R67W

C. Rau No. 1
SE 1/4 SW 1/4 sec 35, T139N, R68W

Calvert Exploration Co.
NDGS No. 670

Calvert Exploration Co.
NDGS No. 672

Calvert Exploration Co.
NDGS No. 673

D. C. Wood No. 1
SE 1/4 SW 1/4 sec 24, T139N, R67W

V. Wanzek No. 1
NW 1/4 NW 1/4 sec 12, T139N, R67W

F. L. Robertson No. 1
NE 1/4 NE 1/4 sec 26, T138N, R67W

WARD COUNTY

Stanolind Oil and Gas Co.
NDGS No. 105

Quintana Production Co.
NDGS No. 126

W. H. Hunt
NDGS No. 588

Anschutz Corp., Inc. et al.
NDGS No. 4990

W. & I. Waswick No. 1
SW 1/4 NE 1/4 sec 2, T153N, R85W

C. W. Linnerte No. 1
SW 1/4 SE 1/4 sec 33, T156 N, R83W

F. C. Neumann No. 1
SW 1/4 SE 1/4 sec 33, T152N, R82W

R. Musch No. 1
NW 1/4 SW 1/4 sec 22, T156N, R84W

WELLS COUNTY

Continental Oil Co.
NDGS No. 207

C. Hunt Trust Estate
NDGS No. 609

C. Hunt Trust Estate
NDGS No. 689

Calvert Drilling Inc.
NDGS No. 1211

Lueth No. 1
SE 1/4 SE 1/4 sec 27, T146N, R73W

G. Leitner No. 1
SW 1/4 SE 1/4 sec 14, T148N, R71W

N. Thorndodssard No. 1
NE 1/4 NE 1/4 sec 31, T147N, R71W

F. Zwinger No. 1
NE 1/4 NE 1/4 sec 8, T146N, R68W

WILLIAMS COUNTY

Texaco Inc.
NDGS No. 999

Amerada Petr. Corp.
NDGS No. 1231

Amerada Petr. Corp.
NDGS No. 1385

Amerada Petr. Corp.
NDGS No. 1403

Amerada Petr. Corp.
NDGS No. 1636

Amerada Petr. Corp.
NDGS No. 4321

Amerada Petr. Corp.
NDGS No. 4323

Amerada Petr. Corp.
NDGS No. 4618

L. Hunt
NDGS No. 4916

Amerada Hess Corp.
NDGS No. 5912

J. M. Donahue No. 1
SW 1/4 NE 1/4 sec 23, T154N, R100W

Beaver Lodge Ord. No. 1
NE 1/4 sec 2, T155N, R96W

N.D. "A" No. 9
C SW 1/4 sec 16, T156N, R95W

Beaver Lodge Dev. No. B304
NE 1/4 SW 1/4 NE 1/4 sec 15, T155N,
R96W

B.L.O.U. No. 2
SW 1/4 sec 17, T156N, R95W

N.D. "C" "B" No. 9
NW 1/4 SW 1/4 sec 36, T158N, R95W

Lalim-Ives No. 1
NE 1/4 SW 1/4 sec 26, T158N, R95W

N. Trossstad No. 1
NE 1/4 NW 1/4 sec 17, T156N, R103W

P. Haarstad No. 1
NE 1/4 SW 1/4 sec 29, T156N, R102W

B.L.O.U. No. 6
NE 1/4 SW 1/4 sec 35, T156N, R96W

RICHLAND COUNTY, MONTANA

Shell Oil Co.

Swigart No. 24X-8
sec 8, T22N, R60E

APPENDIX B

Log picks of the tops of the various units in the upper Red River. Depth in feet measured from the kelly bushing.

NDGS WELL NO.	6050	632	291	555	2853	3268	3746	4254	5195	6169	6303	38	286	4655	485	516
K.B.	2695	1637	2774	2815	2572	2540	2814	2864	2786	2555	2642	1526	1539	1486	3212	3074
Red River	9018	4291	12220	13115	12774	11901	12001	11627	11694	12766	12782	7239	5735	5950	9156	10397
A porous zone						11916						7255	5750		9169	10408
A basal limestone						11930						7265			9180	10420
B anhydrite					12822	11946						7275	5755			10436
B porous zone					12838	11952						7285	5760		9199	10440
B basal limestone					12858	11964						7305	5785		9212	10453
C anhydrite		4348	12321	13228		12004	12102	11721	11792	12875	12888	7320	5800	6020	9249	10488
C porous zone					12906	12034						7352			9273	10511
C basal limestone					12948	12062									9319	10538
D zone					12976	12071									9345	
Lower Red River		4470	12460	13362			12254	11862	11942	13004	13018	7440		6128	9404	

NDGS WELL NO.	1446	1575	2509	2677	3150	3261	3312	3514	3720	3798	4143	4158	4248	4538	4545	4577
K.B.	3028	2953	2979	3034	3001	2925	2865	2937	3018	3037	3179	2952	2969	3145	2865	3211
Red River	9278	8198	8151	8114	8418	8244	8194	8265	8314	8634	9462	8200	8220	9340	9658	9121
A porous zone	9286	8210	8167	8131	8434	8259	8209	8280	8332	8648	9472	8219	8234	9349	9665	9132
A basal limestone	9298	8222	8180	8144		8271	8221	8292	8342	8660	9481	8228	8240	9360	9675	9141
B anhydrite	9310	8235	8190	8208	8455	8287	8234	8307	8357	8676	9499	8239	8257	9379	9694	
B porous zone	9316	8240	8193	8212	8459	8291	8238	8310	8360	8679	9504	8243	8260	9382	9696	9160
B basal limestone	9333	8249	8206	8220	8468	8299	8246	8316	8368	8686	9514	8254	8269	9393	9704	9173
C anhydrite	9365	8284	8243	8257	8508	8338	8285	8358		8730	9550	8296		9429	9741	9211
C porous zone	9386	8304	8272	8273	8530	8359	8309	8371		8751	9567	8318		9452	9766	9237
C basal limestone	9413		8289	8307	8561	8405	8326	8407		8792	9600	8359		9480	9800	9276
D zone	9447		8313	8338	8594	8424	8351	8441		8809	9641	8379		9521	9823	9301
Lower Red River	9522	8440	8384	8404	8640	8492	8429	8493		8857	9699	8429		9580	9895	9362

NDGS WELL NO.	4641	4654	4662	4669	4756	4821	4832	4841	4922	4932	4952	4954	5000	5045	5061	5070
K.B.	3197	2935	3252	3158	3201	3116	3137	3246	2944	3160	2958	3160	2977	3242	3125	2960
Red River	9416	9430	9191	9605	9150	9345	9377	9148	9779	9426	9570	9428	8958	9480	9394	9222
A porous zone	9427	9438	9200	9616	9162	9358	9386	9160	9784	9430	9577	9439	8970	9490	9404	9236
A basal limestone	9438	9445	9211	9628	9168	9370	9399	9167	9794	9438	9586	9448	8986	9496	9422	9249
B anhydrite	9456		9225	9642	9188	9383		9184	9814	9453	9606	9470	9003	9516	9439	9271
B porous zone	9459	9472	9227	9647	9194	9386	9420	9187	9819	9459	9611	9472	9006	9519	9443	9274
B basal limestone	9471	9478	9240	9655	9202	9396	9428	9200	9826	9470	9618	9481	9015	9527	9449	9280
C anhydrite	9506		9275	9691	9240	9434	9467	9239	9861	9508	9656	9520	9055	9568	9487	9318
C porous zone	9529	9515	9300	9712	9252	9457	9483	9262	9885	9528	9680	9538	9076	9588	9498	9338
C basal limestone	9556	9564	9328	9746	9296	9484	9512	9296	9904	9558	9708	9577	9112	9620	9540	9380
D zone	9599	9606	9345	9776	9327	9521	9556	9326	9945	9588	9739	9608	9146	9656	9574	9408
Lower Red River	9658	9668	9417	9842	9390	9585	9611	9390	10018	9663	9815	9675	9202	9718	9643	9468

APPENDIX B (Cont'd)

Log picks of the tops of the various units in the upper Red River. Depth in feet measured from the Kelly bushing.

NDCS WELL NO.	5089	5128	5133	5163	5200	5209	5227	5256	5262	5266	5269	5270	5278	5347	5382	5397
K.B.	3137	3089	3258	3240	3135	3029	2938	3207	2934	3207	3185	2992	3255	3042	3199	3091
Red River	9412	9122	9579	9696	8938	9348	8916	9652	8937	9497	9616	8991	9594	9623	9143	9555
A porous zone	9424	9136	9588	9706	8951	9356	8922	9664	8946	9508	9627	9000	9604	9634	9153	9559
A basal limestone	9433	9143	9595	9717	8958	9365	8928	9672	8952	9518	9636	9011	9610	9644	9163	9568
B anhydrite	9448		9611	9735	8976	9384	8947	9639	8968	9536	9651	9029	9632	9665	9181	9592
B porous zone	9452	9154	9619	9738	8978	9389	8950	9644	8972	9540	9656	9032	9635	9669	9185	9596
B basal limestone	9459	9168	9630	9746	8990	9397	8960	9702	8983	9548	9666	9039	9645	9674	9197	9604
C anhydrite	9498	9206	9670	9784	9030	9435	8997	9740	9021	9587	9703		9682	9714	9233	9642
C porous zone	9512	9225	9689	9806	9052	9450	9015	9763	9042	9600	9725	9075	9696	9731	9254	9660
C basal limestone	9548	9260	9727	9841	9102	9475	9046	9791	9082	9628	9758	9144	9734	9766	9289	9693
D zone	9590	9297	9750	9866	9124	9500	9092	9828	9106	9670	9787	9164	9766	9796	9327	9722
Lower Red River	9648	9355	9823	9935	9185	9574	9147	9890	9171	9729	9854	9222	9838	9863	9382	9791

NDCS WELL NO.	5402	5403	5421	5456	5459	5492	5495	5567	5584	5618	5651	5700	5712	5733	5745	5772
K.B.	2889	2967	3145	3107	2916	3223	3015	3008	2888	2954	3105	3052	2915	2832	3244	2892
Red River	9156	8922	9392	9270	9440	9112	9225	8361	9288	9055	9258	8920	9388	9204	9784	10053
A porous zone	9162	8930	9403	9284	9450	9124	9235	8373	9248	9065	9613	8926	9396	9212	9796	10063
A basal limestone	9172	8936	9412	9289	9460	9132	9245	8382	9304	9074	9626	8934	9405	9217	9804	10073
B anhydrite	9193		9430	9310				8399	9329		9643	8952	9422	9244	9823	10092
B porous zone	9196	8960	9434	9312	9484	9152	9266	8401	9333	9093	9647	8956	9429	9247	9828	10098
B basal limestone	9202	8966	9444	9320	9491	9164	9275	8409	9340	9098	9658	8966	9437	9253	9837	10106
C anhydrite	9235		9480	9355	9529	9204	9310	8448	9375	9136	9692	9002	9473	9267	9876	10143
C porous zone	9256	9000	9502	9374	9558	9226	9336	8462	9396	9151	9716	9027	9488	9309	9898	10167
C basal limestone	9280	9038	9532	9405	9577	9264	9364	8492	9423	9172	9745	9042	9526	9327	9931	10193
D zone	9325	9074	9576	9448	9624	9296	9399	8536	9470	9220	9780	9071	9572	9378	9962	10225
Lower Red River	9384	9136	9631	9506	9678	9366	9465	8590	9523	9273	9841	9133	9627	9438	10022	10282

NDCS WELL NO.	5823	5829	5865	5882	5892	5895	5904	5709	5920	5951	5967	6074	155	174	701	723
K.B.	2961	3195	2918	3052	3193	2919	3043	2921	2960	3030	3039	2850	1901	1910	2023	1877
Red River	9558	9529	9333	8997	9463	9446	9700	9437	9472	9263	8928	9224	5080	5775	5400	5030
A porous zone	9565	9538	9340	9009	9473	9454	9713	9444	9481	9268	8941	9230		5800		
A basal limestone	9571	9544	9349	9016	9482	9460	9721	9453	9488	9278	8944	9239		5810		
B anhydrite	9594	9570	9368	9034	9502	9486	9740	9478		9297	8969	9262				
B porous zone	9597	9575	9372	9038	9505	9488	9746	9481	9512	9300	8972	9266		5816		
B basal limestone	9601	9585	9382	9050	9516	9494	9757	9487	9518	9313	8982	9273		5825		
C anhydrite		9622	9420	9089	9553	9535	9798	9524	9556	9348	9017	9307		5838		
C porous zone	9639	9637	9442	9116	9576	9558	9822	9547	9570	9371	9044	9332		5850		
C basal limestone	9679	9667	9466	9146	9602	9610	9874	9573	9612	9400	9064	9348		5894		
D zone	9725	9702	9514	9170	9636	9634	9880	9624	9639	9425	9104	9394		5905		
Lower Red River	9779	9768	9570	9241	9706	9691	9956		9702	9499	9166	9450	5230	5960	5582	5186

APPENDIX B (Cont'd)

Log picks of the tops of the various units in the upper Red River. Depth in feet measured from the kelly bushing.

NDGS WELL NO.	756	763	765	772	1546	2010	4837	5192	5248	505	793	3044	4220	4611	4725	4957
K.B.	1890	1947	2027	2007	2261	2195	2112	2373	2242	2296	2102	2200	2210	2435	2373	2212
Red River	5313	6060	5876	6361	11131	10390	10728	11182	10880	12313	13014	12020	13014	13771	14240	13360
A porous zone					11160					12330		12047	13044			13394
A basal limestone					11172					12335		12049	13051			13397
B anhydrite										12362		12076	13074	13828		13429
B porous zone				6386	11203					12374		12092	13087	13842		13438
B basal limestone				6393	11212					12380		12104	13100	13853		13454
C anhydrite		6124		6438	11250	10494	10830	11270	10979	12424	13190	12140	13139	13891		13488
C porous zone		6140		6454						12442	13206		13158	13922		13524
C basal limestone		6190		6496						12469	13266		13188	13950		13544
D zone											13284		13222	13972		13572
Lower Red River	5500	6244	6040	6566	11362	10618	10946	11382	11098				13276	14032		13615

NDGS WELL NO.	5621	5887	5971	6086	16	23	43	287	403	410	4130	5438	3636	5097	5118	5496
K.B.	2583	2203	2360	2327	1909	2012	1820	1513	1547	2513	2867	2710	2350	2512	2194	2408
Red River	12796	12460	13324	13250	4290	4470	4750	2290	2818	12400	11032	11558	8662	7580	7026	9065
A porous zone		12487	13356	13284									8666			9068
A basal limestone		12491	13367	13294									8675			9078
B anhydrite	12854	12514	13382	13310									8699	7611	7051	9101
B porous zone	12859	12528	13398	13323									8704	7615	7054	9106
B basal limestone	12866	12541	13412	13337									8716	7630	7068	9117
C anhydrite	12902	12575	13450	13372			4820			12505	11134	11664	8762	7673	7113	9170
C porous zone	12927	12614	13486	13406									8778	7698	7136	9200
C basal limestone	12971	12641	13522										8812	7741		9228
D zone	12990	12676	13540										8834	7768	7192	9258
Lower Red River	13052		13608		4450	4615		2460	2995	12640	11283	11811		7811	7250	

NDGS WELL NO.	511	4984	5447	24	230	748	590	5523	39	61	956	2373	2584	2602	3645	3084
K.B.	2614	2524	2430	1968	1890	1848	2011	2117	1480	1570	2339	2117	2463	1983	2379	2344
Red River	10208	9844	9974	4582	4235	5026	4312	4240	6350	6338	12763	13109	13022	12920	12184	13478
A porous zone	10221	9851	9990								12789	13148				
A basal limestone	10229	9860									12798	13152				
B anhydrite	10249	9884	10010								12821	13174				
B porous zone	10253	9890	10020								12834	13186				
B basal limestone	10266	9900	10029								12849	13204				
C anhydrite	10301	9948	10080	4640	4286						12890	13240	13128	13040	12300	13606
C porous zone	10320	9973	10100	4650	4290						12905	13268		13079		
C basal limestone		10000	10122	4690							12944			13104		
D zone		10030	10146	4700							12956			13121		
Lower Red River		10072		4766	4424	5187	4489	4380	6545	6530	13020	13356	13273	13154	12445	13728

APPENDIX B (Cont'd)

Log picks of the tops of the various units in the upper Red River. Depth in feet measured from the kelly bushing.

NDGS WELL NO.	4062	4305	4723	4807	5002	5655	5821	5840	49	21	1620	3859	3978	5379	4386	5072
K.B.	2214	2515	2048	2130	2372	2170	2128	2103	2081	2284	2426	2124	2281	1980	2216	2367
Red River	13336	12576	13416	13588	12770	12751	12355	12744	7996	11160	10341	6920	7048	6527	12810	11600
A porous zone												6926				
A basal limestone												6933				
B anhydrite									8034			6951				
B porous zone					12840				8045			6957				
B basal limestone									8060			6973				
C anhydrite	13450	12688	13530	13705	12880	12871	12470	12868	8078		10456	7008	7147	6610	12938	11689
C porous zone					12890	12894	12485	12887	8105			7028				
C basal limestone					12917		12519									
D zone					12982											
Lower Red River	13612	12836	13702	13844			12588		8250		10579	7140	7288	6739	13066	11804

NDGS WELL NO.	15	95	4940	435	706	3920	316	665	684	693	735	631	91	3383	3588	4075
K.B.	2033	1924	2231	1589	1641	1596	1680	1793	1849	1984	1994	1730	2801	2787	2895	2777
Red River	7644	7400	9307	3992	4200	5123	4180	5954	5544	6270	5500	5050	11046	9147	9894	11241
A porous zone	7656					5130								9162	9913	
A basal limestone	7660					5134								9172	9918	
B anhydrite	7685													9184		
B porous zone	7694					5149								9190	9938	11287
B basal limestone	7707					5166								9203	9948	11298
C anhydrite	7732	7475	9405			5183				6334	5552	5122	11147	9241	9985	11338
C porous zone	7748					5210				6354	5558	5128		9266	10007	11363
C basal limestone	7822					5242				6406	5625	5190		9296	10053	11396
D zone						5270								9326	10073	11424
Lower Red River	7874			4150	4365	5300	4345		5740	6458	5690	5236	11300	9370	10114	11482

NDGS WELL NO.	4124	4241	4280	4749	5210	5933	850	3515	4134	4182	4311	5142	5143	5255	40	134
K.B.	2729	2868	2971	2976	2975	2897	2650	2277	2341	2344	2560	2326	2688	2717	1857	1551
Red River	11273	11325	10787	10443	10678	10341	11894	11430	10165	10162	11969	10260	11612	11258	3220	2540
A porous zone		11342	10798				11908		10173	10168						
A basal limestone		11349	10808				11917		10176	10174						
B anhydrite		11367	10820				11468		10201	12014						
B porous zone	11319	11370	10829				11948	11482	10218	10211	12022					
B basal limestone	11330	11380	10838				11958	11496	10227	10224	12035					
C anhydrite	11369	11424	10880		10767	10427	11994	11529	10268	10265	12072	10365	11712	11363		
C porous zone	11388	11446	10902				12027	11546	10282	10282	12102					
C basal limestone	11417	11475	10941					11573	10310	10309	12136					
D zone	11438	11492	10976					11596	10335	10334	12160					
Lower Red River	11496	11564	11010		10914	10565	12146	11660	10408	10408		10492			3350	2700

APPENDIX B (Cont'd)

Log picks of the tops of the various units in the upper Red River. Depth in feet measured from the kelly bushing.

NDGS WELL NO.	668	669	670	672	673	105	126	588	4990	207	609	689	1211	999	1231	1385
K.B.	1907	1880	1874	1867	1919	2175	1772	2086	1788	1933	1601	1702	1608	2253	2316	2360
Red River	2817	3172	2940	3002	2897	10082	8660	8815	9034	5032	4220	4404	3510	13858	12670	13128
A porous zone						10105								13889		
A basal limestone						10115								13902		
B anhydrite						10136								13922	12726	
B porous zone						10144								13928	12732	
B basal limestone						10160								13946	12758	
C anhydrite						10190	8750	8900	9086	5084	4280	4462		13977	12772	13248
C porous zone						10215					4286			13994	12784	
C basal limestone											4330		3640		12826	
D zone											4360		3656		12847	
Lower Red River	2994	3336	3117	3166	3088	10340	8905	9070	9262	5214	4430	4602	3713		12874	13352

NDGS WELL NO.	1403	1636	4321	4323	4618	4916	5912	M.T.								
K.B.	2165	2401	2457	2460	2413	2409	2294	2183								
Red River	12658	12992	12725	12589	12766	13215	12794	12387								
A porous zone	12686															
A basal limestone	12702															
B anhydrite	12720					13290		12462								
B porous zone	12726					13299		12474								
B basal limestone	12734					13312		12480								
C anhydrite	12774	13115	12790	12702	12883	13338	12906	12512								
C porous zone	12808					13348		12536								
C basal limestone	12832					13368										
D zone	12854					13408		12579								
Lower Red River	12884	13204	12948	12800	13000		13022									